Magnetic Force Microscopy (MFM) Characterization of Superparamagnetic Nanoparticles (SPIONs)

by

Gustavo Cordova

A thesis
presented to the University of Waterloo
in fulfillment of the
thesis requirement for the degree of
Master of Science
in
Biology - Nanotechnology

Waterloo, Ontario, Canada, 2012

Author's Declaration

I hereby declare that I am the sole author of this thesis. This is a true copy of the thesis, including any required final revisions, as accepted by my examiners. I understand that my thesis may be made electronically available to the public.

Abstract

Superparamagnetic iron oxide nanoparticles (SPIONs), due to their controllable sizes, relatively long *in vivo* half-life and limited agglomeration are ideal for biomedical applications such as magnetic labeling, hyperthermia cancer treatment, targeted drug delivery and for magnetic resonance imaging (MRI) as contrast enhancement agents. However, very limited studies exist on detecting and characterizing these SPIONs *in vitro* in physiologically relevant conditions. It would be of interest to localize and characterize individual SPIONs at the nanoscale in physiologically relevant conditions. MFM offers great potential for this purpose. We evaluate the applicability of Magnetic Force Microscopy (MFM) in air as well as in liquid to characterize bare and SiO_2 coated SPIONs on mica .The magnetic properties of bare and SiO_2 coated SPIONs are compared on the nanoscale using MFM. MFM phase- shift dependence on scan height is investigated using SPION samples that have been coated in hydrophobic polymers, polystyrene (PS) and poly (methyl methacrylate) (PMMA). The polymers are used to spin-coat SPION samples and mimic cell lipid bilayers. Nanoscale MFM images of SPIONs in a liquid environment, covered with these hydrophobic polymers are also presented for the first time. The use of 3-merceptopropyltrimethoxysilane (3-MPTS) to covalently attach SiO_2 SPIONs to gold substrates for the potential purpose of MFM imaging in liquid is also briefly addressed. These results will allow us to understand the feasibility of detecting magnetic nanoparticles within cell membranes without any labeling or modifications and present MFM as a potential magnetic analogue for fluorescence microscopy. These results could be applied to cell studies and will lead to a better understanding of how SPIONs interact with cell membranes and have a valuable impact for biomedical applications of all types of magnetic nanoparticles.

Acknowledgments

I would like to take this opportunity to thank the many people who have supported me through this project. I sincerely thank my supervisors Dr. Zoya Leonenko and Dr. Frank Gu for their support throughout this thesis. I thank Frank for his time, patience and shared experience throughout the last two years. I am grateful to Zoya for the opportunity to have been part of her lab and for all that she has taught me, both as a scientist and as a person. Her positive attitude and encouragement made this degree a reality. I would also like to thank Dr. Ravi Gaikwad and Dr. Simon Attwood, the postdoctoral fellows in Zoya's lab group. Their constant optimism, kindness and expertise in the lab were invaluable and truly made this degree possible. They were always there to answer my many questions and remind me to be positive and truly made me feel welcome in the lab. They have been true friends throughout this process, sharing their knowledge and experience whenever I needed it. I would also like to thank everyone in the Leonenko lab group. I could not have asked for a better lab group to share this time with. A final thank you to the entire Biology department, especially administration both past and present, for this wonderful experience and all the fond memories.

Table of Contents

AUTHOR'S DECLARATION ..... **ii**

ABSTRACT ..... **iii**

ACKNOWLEDGMENTS ..... **iv**

TABLE OF CONTENTS ..... **v**

LIST OF FIGURES ..... **viii**

LIST OF TABLES ..... **ix**

LIST OF ABBREVIATIONS ..... **x**

CHAPTER 1: INTRODUCTION

1.1 Biomedical Applications of SPIONs **1**

1.1.1 MRI Contrast Agents 1

1.1.2 Magnetic Cell Separation and Labeling 3

1.1.3 Targeted Drug Delivery 5

1.2. Magnetic Resonance Imaging (MRI) **8**

1.2.1 Principle and Method 8

1.2.2 Superparamagnetism 10

1.3 Methods for SPION Synthesis **13**

1.3.1 Co-precipitation in an Aqueous Medium 14

1.3.2 Hydrothermal and Sol-gel Methods 15

1.3.3 Reverse Microemulsion Method 16

1.3.4 Stabilization, Colloid Stability and Surface Modification of SPIONs 17

1.3.4.a Steric Stabilization *18*

1.3.4.b Electrostatic Stabilization *19*

1.3.4.c SiO_2 Coated SPIONs 20

1.4 Characterization of SPIONs 22

1.4.1 Physical Characterization 22

1.4.2 Magnetic Characterization 24

1.4.2.a MFM Characterization of SPIONs 26

CHAPTER 2: RESEARCH OBJECTIVES

2.1 Motivations for Study 29

2.2 Rationale for Experiments 31

CHAPTER 3: MATERIALS AND METHODS

3.1 Atomic Force Microscopy (AFM) 36

3.2 Magnetic Force Microscopy (MFM) 37

3.3 Experimental Section 39

3.3.1 SPION Synthesis 39

3.3.2 SPION Deposition on Bare Mica 40

3.3.3 PS and PMMA coated sample preparation 40

3.3.4 Substrate (mica) modification via 3-MPTS 41

3.3.5 MFM Imaging 43

CHAPTER 4: RESULTS AND DISCUSSION 44

4.1 Methods for Securing SPIONs to Substrate in Liquid 44

4.2 Bare vs. SiO_2 Coated SPIONs 47

4.3 MFM Phase-shift Dependence on Scan Height 51

4.4 MFM of SPIONs in Liquid 55

4.5 SPIONs on 3-MPTS Functionalized Gold 57

CHAPTER 5: CONCLUSIONS AND FUTURE STUDIES 60

REFERENCES 62

List of Figures

Figure 1.1: Immunoselection demonstrating positive selection of T cells using magnetic nanoparticles 4

Figure 1.2: Illustration of proton magnetic moments in the absence a) and presence b) of perpendicular time varying magnetic fields for MRI 9

Figure 1.3: MRI of a mouse brain enhanced by iron oxide nanoparticles 10

Figure 1.4: Comparison of ferromagnetic and superparamagnetic hysteresis loops 25

Figure 2.1: Deposition of SiO_2 coated SPIONs via (3-MPTS)..... 34

Figure 3.1: Schematic of AFM and MFM imaging techniques 38

Figure 4.1: AFM topography image of SPIONs with PLL on mica 45

Figure 4.2: Characterization of bare vs. SiO_2 coated SPIONs 48

Figure 4.3: MFM phase-shift vs. particle size for bare and SiO_2 coated SPIONs..... 50

Figure 4.4: MFM phase-shift vs. lift height data for SiO_2 coated SPIONs covered with PS... 52

Figure 4.5: MFM in liquid image of SiO_2 coated SPIONs spin-coated with PMMA..... 55

Figure 4.6: Comparison of SPIONs in water or TMAOH solvent on gold coated 3-MPTS functionalized mica 58

List of Tables

Table 1.1: Critical diameter values for some common magnetic nanoparticles.....11

List of Abbreviations

3-MPTS	3-mercaptopropyltrimethoxysilane
AFM	atomic force microscopy
CVD	chemical vapour deposition
DLS	dynamic light scattering
DOPC	dioleyl phosphatidyl choline
EXAFS	extended x-ray absorption of fine structures
FC	field cool
FDA	food and drug administration
MBE	molecular beam epitaxy
MFM	magnetic force microscopy
MPS	mononuclear phagocyte system
MRI	magnetic resonance imaging
NMR	nuclear magnetic resonance
PCS	photonic correlation spectroscopy
PEG	poly-ethylene glycol
PLGA	polylactic-co-glycolic acid
PLL	poly-L-lysine
PMMA	poly (methyl methacrylate)
PS	polystyrene
PVP	polyvinylpyrrolidone
PVA	polyvinyl alcohol
SEM	scanning electron microscopy
SPIONs	superparamagnetic iron oxide nanoparticles
SQUID	superconducting quantum interference device
TEM	transmission electron microscopy
TEOS	tetraethylorthosilicate
TMAOH	tetramethylammonium hydroxide
XRD	x-ray diffractograms
ZFC	zero field cool

1.0 Introduction

1.1 Biomedical applications of SPIONs

Biocompatible superparamagnetic iron oxide nanoparticles (SPIONs) have been widely used for biomedical applications such as tissue specific release of therapeutic agents, magnetic hyperthermia treatment for cancer patients and a wide range of cell separation techniques. Yet, very few studies exist with the purpose of detecting or imaging SPIONs *in vitro* or in cell-like systems at physiologically relevant conditions. This type of study is important considering the ubiquitous prevalence of these SPIONs in the field of biomedicine.

1.1.1. MRI contrast agents

Most often SPIONs are used as magnetic resonance imaging (MRI) contrast enhancement agents. They are intravenously infused into the body to detect and characterize small lesions or tumours in organs or to visualize the digestive tract (Laurent *et al.*, 2010). These SPION contrast agents, such as Feridex I.V., Endorem, Combidex, and Sinerem are commercially available through several biotechnology companies and have all been FDA approved for use with MRI patients (Mahmoudi *et al.*, 2010). Contrast agents used in MRI shorten or enhance the T_1 and T_2 relaxation rates, longitudinal and transverse respectively, of the surrounding hydrogen atoms to the extent that there will be a measurable difference or contrast between the tissues that are bound to contrast agents and those that are not (Goya *et al.*, 2008). Typically, SPION contrast agents shorten the T_2 relaxation rates and allow MRI to differentiate between different organs in the body but primarily benign and malignant tissues (Goya *et al.*, 2008). Due to their high magnetization, SPIONs cause a critical decrease in the relaxation rate of water protons, and are

therefore efficient MRI contrast agents. Iron oxide nanoparticles are used most commonly for this purpose due to their low toxicity, chemical stability and biocompatibility. SPIONs can be processed by cells using well characterized iron metabolism pathways and thus have received FDA approval to be used safely in humans (Pankhurst *et al.,* 2009). SPIONs injected into the body are recognized as foreign invaders. Subsequently, the mononuclear phagocyte system (MPS) attempts to remove them from circulation through opsonization and phagocytosis by macrophages (Owens *et. al.,* 2006). SPIONs approximately 50nm and larger are typically opsonized quickly upon being injected into the body which leads to their significant phagocytosis by macrophages, specifically Kupffer cells (Laurent *et al*., 2010). This is the main advantage of SPIONs of this size. Ultra-small SPIONs, similar to the particles being used in this thesis study, are below 50nm in diameter (typically 10-30nm). As a result, they have a much longer half-life in the blood and are more efficient MRI contrast agents. Due to the smaller surface area of the nanoparticle, opsonins will bind less efficiently to the particle. Studies have shown that ultra-small SPIONs are progressively taken up by macrophages in healthy lymph nodes and consequently are very effective when used for MRI of lymph nodes (Pultrum *et al.,* 2009). When injected, the majority of SPIONs and other contrast agents will undergo hepatic capture. Subsequently, the application of these particles when they are uncoated (e.g., with vectorizing agent or neutral coating) is restricted to imaging tissues in the mononuclear phagocyte system such as the liver and any metastases associated with it (Laurent *et al*., 2010).

Core-shell magnetic nanoparticles have also shown great potential as MRI contrast agents due to their highly functional surfaces that demonstrate great potential for ligandization with target antigens and receptors. SPIONs coated with a silicon oxide (SiO_2) shell, like those used in this study, have applications in a wide range of therapies and have shown relaxivity values

comparable to those of metal, alloy and spinel magnetic nanoparticle contrast agents (Kim *et al.*, 2008). It is necessary for any type magnetic nanoparticle used as a contrast agent to have high values of magnetization which cause higher contrast and ultimately require a smaller amount of nanoparticles to be injected.

1.1.2. Magnetic cell separation and labeling

SPIONs are also used extensively to label and separate biological entities such as cells, DNA and proteins. Magnetic separation is fundamentally different from most methods used to separate biologically important substances, such as centrifugation and filtration, as it does not rely on physical or chemical differences between the entities being separated. Instead, it relies on the tagging of these biological entities with SPIONs and the subsequent exposure of these tagged entities to varying magnetic fields. Often these biological entities are labeled with appropriate antibodies before being bound to the magnetic nanoparticles. In a typical cell separation, the cell suspension is incubated with the magnetic nanoparticles along with the appropriate antibodies, and then is exposed to a magnetic field and finally is washed to remove any untagged cells. The tagged cells can then be re-suspended and collected. Figure 1 illustrates the positive selection of T cells in immunoselection.

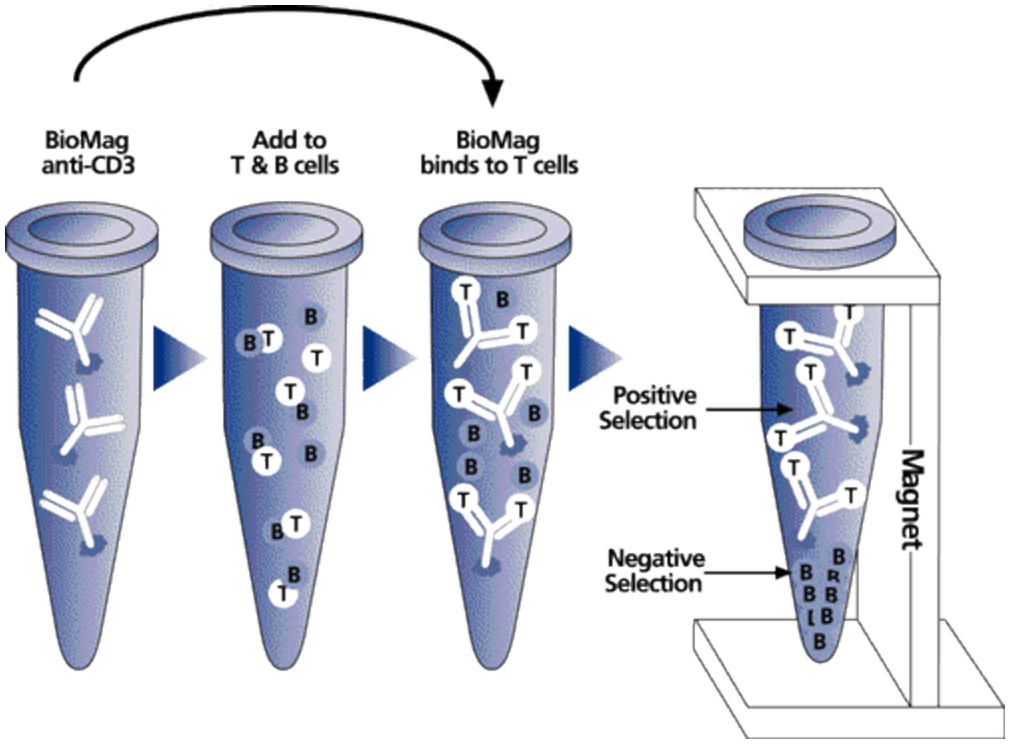

Figure 1.1. Immunoselection demonstrating positive selection of T cells using magnetic nanoparticles (Vettese-dadey, 1999).

In the above figure, BioMag is the antibody which coats the magnetic nanoparticle and binds to the T cells in solution. Magnetic separation has proven to be a successful technique in research as well as therapeutics, mostly due to its high sensitivity and ability to separate a low number of target entities (Liberti *et al.*, 2001). This has led to its use in the separation of rare tumour cells from blood and the detection of malarial parasites in blood (Paul *et al.*, 1981). A study in 2002 by Hoffman *et al.* used magnetic separation as pre-processing technology to identify and amplify DNA within a polymerase chain reaction sample. Cell counting techniques able to determine the number and location of tagged cells have also been developed using magnetic nanoparticles and magnetic separation (Delgratta *et al.*, 1995). Most recently, SPIONs have been used for biodetoxification of water samples in a lab setting.

1.1.3. Targeted drug delivery

The magnetic properties of superparamagnetic nanoparticles also show potential for exciting therapeutic techniques. Magnetic drug delivery has become a popular concept because it allows for the direct delivery of drugs to their site of action. Most literature that discusses targeted drug delivery cites the advantage of these nanoparticles over traditional chemotherapeutics. Chemotherapeutics are typically administered intravenously which leads to general systemic distribution ultimately leading to deleterious side effects when the drugs attack normal healthy cells as well as cancer cells (Pankhurst *et al.*, 2003). For magnetically targeted cancer therapy applications, a cytotoxic drug is typically attached to a magnetic nanoparticle vehicle. The drug is injected into the patient intravenously, often in the form of a ferrofluid. As shown by Alexiou *et al.*, when the particles reach their target site the cytotoxic drug can be released in a number of ways including enzymatic activity, or a change in pH, osmolality or temperature. In addition, magnetic drug delivery has many therapeutic applications outside of cancer treatment including gene vectorization, DNA therapy, and the delivery of growth promoters to help repair lesions in the central nervous system (Laurent *et al*., 2010).

Targeted drug delivery makes it possible to increase the concentration of drug delivered to the targeted site while reducing the total amount of drug delivered, and consequently, unwanted side effects. This technique relies on the most fundamental advantage of magnetic nanoparticles; they obey Coulomb's Law and can thus be transferred through an external magnetic field gradient. The force on the magnetic particle is proportional to the gradient of the magnetic field being used. High gradient magnetic fields allow for the magnetic nanoparticles to be concentrated and maintained near the tumor or target site (Laurent *et al*., 2010). There are many parameters which can influence the efficacy of magnetically targeted drug delivery.

Magnetic field strength, gradient, and the volumetric and magnetic properties of the particle play a large role. Blood flow rate, circulation time as well as physiological conditions like tissue depth to the target site can influence the success of the procedure.

At present, magnetic nanoparticle drug carriers often adopt the core/shell structure. Current research on magnetic drug carriers focuses on new multi-functional surface coatings and the use of large moment magnetic materials for the particle core. The core is typically composed of SPIONs, either Fe_3O_4 or Fe_2O_3, magnetite and maghemite respectively, which is coated with a biocompatible shell such as silica or dextran. The coating on the magnetic core acts as a barrier between the particle and the surrounding environment and can be functionalized by adding various molecules such as carboxyl groups, biotin and other molecules. The functional groups can also be attached to cytotoxic drugs or antibodies specific for an antigen of the target site. Recent research on magnetic carriers by several groups has largely been focused on new polymeric and inorganic coatings for SPIONs. For example, a study in 2001 by Carpenter considered noble metal coatings such as gold for SPION magnetic carriers. Besides iron oxide, alternative materials such as iron, cobalt and nickel are also being used to make magnetic carriers. There are a number of physical limitations associated with magnetically targeted drug delivery including diminished magnetic field strength with increased depth in the body and difficulty circumventing certain tissue structures and vasculature in order to reach the target site (Dobson, 2006). Although numerous animal studies have been published, these limitations have restricted the clinical success of magnetically targeted drug delivery. However, a recent alternative approach to tumour targeting which involves magnetic nanoparticles and the body's own immune system was demonstrated by Muthana *et al*. Tumors have the potential to outgrow their blood supply when they become too large, resulting in an area of avascular necrotic tissue

at the centre of the tumor. This section of the tumour cannot be reached by the cytotoxic drug/carrier complexes in the bloodstream and the necrotic tissue will release chemical signals to attract macrophages, which help restore the blood supply. Muthana *et al* use this process and load the macrophages with iron oxide nanoparticles, placing magnets external to the tumor allowing for the cytotoxic drug to reach the avascular tissue. This research suggests that there is potential to overcome the physical limitations that are involved with magnetically-targeted drug delivery.

1.2 Magnetic resonance imaging

1.2.1 Principle and method

The most common application for SPIONs, including those being used in this study, is as MRI contrast enhancement agents, and thus it is necessary to consider greater detail regarding MRI principles and method. Magnetic resonance imaging relies on the exceptionally large number of protons within the body. Despite the magnetic moment being exceptionally small on each individual proton , there are so many protons available, 6.6×10^{19} per mm^3 of water, that a measurable effect can be observed in the presence of a large magnetic field B_0 (Elster and Burdette, 2001). The signal from the protons can be measured by using resonant absorption and applying a time varying magnetic field perpendicular to $B_{0,}$ and tuned to the Larmor precession frequency specific to the protons. The equation for the Larmor precession frequency for the protons is as follows

$$\omega_0 = \gamma B_0$$

where γ is the gyromagnetic ratio of ^1H protons and is 2.67×10^8rad $s^{-1}T^{-1}$ (Pankhurst *et al.*, 2003). Before the time varying magnetic field is applied perpendicular to B_0, the magnetic moment of the protons, m, precess either parallel or anti-parallel to B_0 as seen in figure 1.2 a). In clinical or research settings the perpendicular radio frequency is applied to B_0 in a pulsating sequence. When this happens, the magnetic moment of the protons oscillating at their characteristic Larmor frequency and precessing around B_0 and in the same direction becomes resonantly excited into the plane perpendicular to that of B_0 as seen in figure 1.2 b). When the radio frequency pulse is removed the magnetic moments of the protons will relax into their original precession and the coherent signal can be measured by pick-up coils in the MRI scanner

(Pankhurst *et al.*, 2003). The signal from the T_1 and T_2 relaxation rates is then enhanced by a factor of 50-100 by the pick-up coils and computer software (Pankhurst *et al.*, 2003). Typically, SPION contrast agents shorten the T_2 relaxation times and allow MRI to differentiate between different organs in the body, primarily benign and malignant tissues (Goya *et al.*, 2008). MRI takes advantage of SPIONs as contrast agents and their ability to create time varying magnetic fields which promote T_2 (or spin-spin) relaxation of protons in the surrounding water molecules.

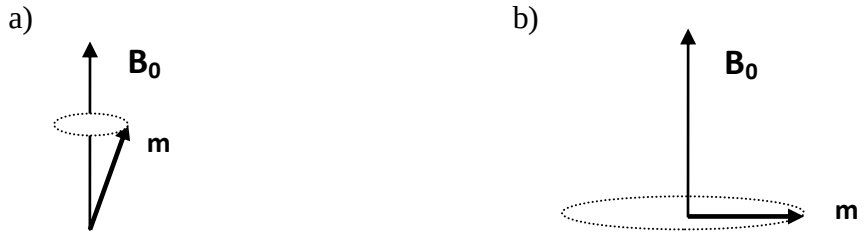

Figure 1.2. Illustration of proton magnetic moments in the absence a) and presence b) of perpendicular time varying magnetic fields for MRI.

The time varying magnetic fields come from both rotational motion of the contrast agent and electron spin flips associated with the unpaired electrons in the superparamagnetic material comprising the contrast agent. These time varying magnetic fields will cause the protons in close proximity to the contrast agents to have an enhanced response (shortened T_2 relaxation time) when exposed to the perpendicular radio frequency pulse. For example in figure 1.3, iron oxide nanoparticles used as contrast enhancement agents 'darken' the MRI signal of a brain tumour implanted into the brain of a mouse (Hadjipanayis *et al.*, 2010).

Figure 1.3. MRI of a mouse brain enhanced by iron oxide nanoparticles. White arrows indicating the tumour in the brain which has been 'darkened' by the contrast enhancement agents (Hadjipanayis *et al.*, 2010).

1.2.2 Superparamagnetism

Superparamagnetism is a phenomenon which occurs in ferromagnetic or ferrimagnetic particles at the nanoscale. In order for a magnetic nanoparticle to reach its superparamagnetic limit, it must first be a single domain particle. A single domain particle is uniformly magnetized with all of the atomic spins aligned in the same direction. Large magnetic nanoparticles adopt a multi-domain magnetic structure, wherein multiple magnetic domains are separated by domain walls. When the size of these particles is reduced to a certain point, it costs more energy to create a domain wall than to support the external stray field energy of the particle. Thus, the magnetic particle adopts a single domain structure. The diameter at which this domain structure change occurs, the critical value or D_c, varies between nanoparticles of different materials (Schuth *et al.*,

2007). Table 1 displays estimated critical diameter values for some common magnetic nanoparticles.

Table 1.1. Critical diameter values for some common magnetic nanoparticles

Material	Critical Value (D_c)
Co	7
Fe	15
Ni	55
Fe_3O_4	128

(Battle *et al.*, 2002)

It is important to note that these estimations are accurate only for spherical particles, and particles with large shape anisotropy will have larger critical diameters (Schuth *et al.*, 2007).

Each single domain magnetic nanoparticle has a magnetic anisotropy energy which causes it to hold its magnetic moment in one of two anti-parallel energetically equal 'easy' axes of magnetization. This magnetic anisotropy energy can be expressed as follows:

$$\mathbf{E(\theta) = K_{eff} V \sin^2 \theta}$$

where V is the particle volume, K_{eff} is the anisotropy constant and θ is the angle between the magnetization and the easy axis (Schuth *et al.*, 2007).The two easy axis directions are separated by an energy barrier that is $K_{eff}V$. When the particle size decreases, the ambient thermal energy k_BT can overcome the energy barrier $K_{eff}V$ and the magnetization of the particle can be easily flipped (Schuth *et al.*, 2007). In situations when the thermal energy exceeds the energy barrier between the two easy axis directions, the particle behaves like a paramagnet in that in the absence of an external magnetic field, the net magnetic moment of the particle appears to be

zero. However, in the presence of an external magnetic field, a giant magnetic moment develops inside of the particle equaling the combined sum of all individual atomic magnetic moments. The resulting particle is known as a superparamagnet. If the experimental time used to measure the magnetization of the particle is longer than the time taken for the particle to flip its magnetization, the particle is said to be in a superparamagnetic state and the net magnetization appears to be zero. If the opposite is true, the particle is said to be in a blocked state and the temperature which separates these two states, the blocking temperature T_B, can be calculated by examining the time frame being used to measure magnetization. Superparamagnets have a magnetic moments and a magnetic susceptibility which is larger than that of paramagnets.

1.3 Methods for SPION synthesis

Magnetite (Fe_3O_4) and maghemite (Fe_2O_3) are the two main groups of iron oxides that comprise SPIONs. Superparamagnetic iron oxide nanoparticles have been synthesized using a number of different methods, including physical, chemical and biological routes. One of the main advantages of SPIONs is their controllable sizes. As a result, there has been a considerable amount of research devoted to the synthesis of magnetic nanoparticles, most recently for the development of efficient synthesis protocols for producing stable, monodisperse and shape-consistent magnetic nanoparticles. Typically, the synthesis of magnetic nanoparticles can be categorized based on the physical state of the starting materials (Goya *et al.*, 2008). The classification scheme consists of two main categories, top-down and bottom-up. In the top-down scheme, the starting material is reduced down to the nanoscale while in the bottom-up scheme, uses atomic or molecular units as building blocks for nanoscale structures (Goya *et al.*, 2008). Common top-down techniques are usually based on physical methods such as mechanical alloying, laser machining and reactive ion etching. Bottom-up techniques include chemical vapor deposition (CVD), molecular beam epitaxy (MBE), and wet routes like sol-gel, microemulsion, and co-precipitation techniques. This section will provide background detail on the most common techniques used for the synthesis of SPIONs as well as the techniques used to synthesize the SPIONs used for this study.

1.3.1 Co-precipitation in an aqueous medium

Co-precipitation is one of the simplest and most commonly used techniques, producing iron oxide nanoparticles (Fe_3O_4 or Fe_2O_3) from an aqueous salt solution containing ferrous and ferric ions, Fe^{2+} and Fe^{3+} respectively, through the addition of an alkaline medium. In this method, precipitation of the ferrous and ferric salts from the solution is the fundamental method of crystallisation and thus the formation of solid nanoparticles via nucleation and crystal growth (Sugimoto, 2000). Once the nuclei of the SPIONs have formed, they are able to uniformly grow in solution by means of further ion diffusion from solution to the surface of the growing nanoparticle. In order for monodispersed SPIONs to form, nucleation must take place followed by uniform crystal growth and then the cessation of further nucleation sites forming. Co-precipitation can be performed in several ways, but for each method the shape, size and composition of the magnetic nanoparticle produced depends on the Fe^{2+}/Fe^{3+} ratio, reaction temperature, pH, and the type of salt being used (chlorides, sulphates or nitrates) (Goya *et al.*, 2008). Many publications refer to a synthesis methods introduced by Massart (Massart, 1980). This method is simple and involves the co-precipitation of ferrous and ferric salts in aqueous medium at the ratio of $0.5Fe^{2+}/Fe^{3+}$ (Hong *et al.*, 2007) (Martinez *et al.*, 2007) (Wu *et al.*, 2007). It produces quasi-spherical magnetite (Fe_3O_4) magnetic nanoparticles in large quantities without using costly materials. These magnetite materials can be easily oxidized using an acidic solution to form maghemite (Fe_2O_3) particles. Massart's method is fast, highly reproducible, economic and can be efficiently carried out on a large scale. Unfortunately, magnetic nanoparticles produced by co-precipitation tend to be polydisperse in nature. Consequently it is difficult to maintain a small nanoparticle size distribution.

1.3.2 Hydrothermal and sol-gel methods

Hydrothermal decomposition has been used to synthesize SPIONs with a smaller size distribution than those produced by co-precipitation (Takami *et al.*, 2007). The hydrothermal method is the oldest reported method for the synthesis of iron oxide nanoparticles. Organometallic precursors, such as iron acetylacetonate or iron carbonates, are thermally decomposed in the presence of different surface surfactants. Typically, hydrothermal decomposition is performed in an aqueous solvent at temperatures above 200ºC. In these conditions, water serves not only as a solvent but also as a catalyst to accelerate the hydrolysis reactions of the organometallic precursors (Laurent *et al.*, 2010). This aqueous method of hydrothermal decomposition is the most prominent in literature, however, Sun *et al.* have synthesized magnetic iron oxide nanoparticles using an organic solvent. Sun and colleagues synthesized these particles by thermally decomposing iron acetylacetonate (III) in the presence of surfactants such as oleic acid, oleyamine and 1,2 – hexadecanediol, and using phenyl and benzyl ether as organic solvents (Sun *et al.,* 2004). In order to produce iron oxide particles with a well-defined radius, Sun *et al.* used a 'seeded growth' procedure in which a small amount of particles, approximately 2nm in diameter, were added to the reaction medium allowing for the production of larger particles (8nm) with a low degree of polydispersity. For the purpose of scaled production, the hydrothermal decomposition method has been built upon to involve the use of microwaves for the synthesis of SPIONs (Khollam *et al.*, 2002).

Sol-gel methods are fundamentally different from hydrothermal methods in that they consist of modifying the precursors to the superparamagnetic nanoparticles at low temperatures. Xu *et al.,* use sol-gel methods to produce ultrafine superparamagnetic powders. Consecutive hydrolysis and condensation reactions of inorganic substances are the basis for these methods,

where slow and controlled reactions generally lead to the formation of small particles (Laurent *et al.,* 2010). Many factors influence the kinetics of the hydrolysis and condensation reactions including pH, temperature, the type of solvent being used, and the concentration of the precursors. For SPIONs requiring a stabilizing surface coating, sol-gel methods make it possible to control the thickness of a silica layer on the surface of the nanoparticle (Laurent *et al.,* 2010).

1.3.3 Microemulsion method

This method, also known as the water in oil (W/O) method, consists of using water droplets, in a continuous oil phase in the presence of surfactants, as nanoreactors in which individual SPIONs are synthesized (Gupta *et al.*, 2004). In the water phase in the centre of the micelles that have formed in the microemulsion, iron precursors can be precipitated as iron oxide. The use of water droplet nanoreactors in a continuous oil phase is advantageous because iron oxide precursors will not precipitate in the organic phase and are only reactive within the micelles in the aqueous phase (Mahmoudi *et al.*, 2010). The main advantage of this method is the strict control over the size of the SPIONs produced. During this process the diameter of the nanoparticles is governed by controlling the size of the nanoreactors and the quantity of precursors available in each emulsion. A microemulsion study by Sun *et al.* in 2004 reported using $Fe(acac)_3$ as an iron source to produce ultra-small SPIONs, 12 and 16 nm in diameter. Limited SPION agglomeration is also achieved by using the microemulsion method due to the surfactants used. Due to how relatively new the microemulsion method is and the large amount of surfactants required to synthesize the SPIONs, this method is currently confined to a laboratory setting.

1.3.4 Stabilization, colloid stability and surface modification of SPIONs

Nanoparticle interactions with themselves and their environment are greatly affected by their surface properties. Application of SPIONs in the fields of research and biomedicine typically requires the nanoparticles to be stabilized via one of several methods of electrostatic or steric stabilization. When stabilizing ferrofluids, the primary goal is to produce a repulsive force between the nanoparticles which will limit nanoparticle agglomerations and provide a stable iron oxide colloid. Co-precipitation typically yields very small SPIONs with very high surface to volume ratios. The small size of these particles forces them to agglomerate in solution, minimizing the interfacial or surface tension between them as well as the free energy of the system. The level of interfacial tension relies on the adsorption of the SPIONs to each other and as a result, the surface properties of the nanoparticles. The aggregation of these SPIONs decreases their value as drug delivery vehicles for biomedical applications lending to their increased size and lower surface area to volume ratios. Therefore, it is important to consider how SPIONs are stabilized in solution by manipulating their surface properties.

Coating nanoparticles with different polymers or functional groups can decrease the interfacial tension between the particles and provide a stable colloid as well as functionalize the SPION surface for further coupling processes. In order for a molecule to be suitable for use as a stabilizing agent, it should be both biocompatible and biodegradable.

1.3.4.a Steric stabilization

Natural or synthetic polymers are generally used to sterically stabilize ferrofluids. These stabilizing agents are either directly involved in the formation process of the nanoparticles or they are used to coat the nanoparticles after they have been formed. The most commonly used molecules as steric stabilizers of SPIONs are surfactants such as oleic acid, lauric acid, alkane sulphonic acids and alkane phosphonic acids (Sahoo *et al.*, 2001). Due to the surfactants' amphiphilic nature, they form a solvation shell around the nanoparticle with the surfactants hydrophobic portion facing outwards. Nanoparticles stabilized in this way must be suspended in an organic solvent and as a result present little potential for biomedical applications or *in vivo* research. Polyelectrolytes, such as alginates or ion surfactants, have also been used to sterically and electrostatically stabilize iron oxide nanoparticles.

Currently, the natural polymer most commonly used to improve the stabilization of SPIONs is dextran. Commercial contrast agents are often made up of iron oxide nanoparticles coated with dextran (Laurent *et al.*, 2010). The hydrogen bonds between the functional groups on the dextran chain interact with the proton sites of the iron oxide nanoparticles, allowing for the adsorption of the dextran onto the nanoparticles. Other natural polymers such as chitosan (Janardhanan *et al.*, 2008), gelatin (Yonezawa *et al.*, 2008), pullulan (Rekha and Sharma, 2007), starch (Miltenyi *et al.*, 1990) and albumin (Saboktakin *et al.*, 2009) have been shown to sterically stabilize iron oxide nanoparticles in solution.

The most prominent synthetic polymer found in literature is poly-ethylene glycol (PEG). Poly-ethylene-glycol is often used because of its hydrophilic nature and biocompatibility with respect to biomedical applications. A study by Schultz *et al.* demonstrated that PEG on the surface of iron oxide nanoparticles not only increased their steric stabilization but also increased

the nanoparticles half life *in vivo* (Schultz *et al.*, 2007). Synthetic co-polymers of PEG such as PEG-poly aspartic acid (PEG-PAsp) have been shown to take part in the formation of stable ferrofluids as well. Various PEG co-polymers have received US Food and Drug Administration approval for use in drug delivery for pharmaceutical companies (Wassel *et al.*, 2007). A wide range of synthetic polymers such as poly (ethylene-co vinyl acetate), polyvinylpyrrolidone (PVP), polylactic-co-glycolic acid (PLGA) and polyvinyl alcohol (PVA) have also been used to stabilize SPIONs in aqueous suspensions (Zhao *et al.*, 1998).

1.3.4.b Electrostatic stabilization

Electrostatic stabilization occurs when the polymers or molecules being used to stabilize the SPIONs in colloidal form are charged. This stabilization relies on charged functional groups, such as carboxylate, sulphonate, phosphonate and sulphate that are able to adsorb onto the SPIONs via substitution of the hydroxy ligands present on the surface of the iron oxide. The adsorption of these functional groups decreases the interfacial tension between the particles by modifying their isoelectric point and consequently improving their colloidal stability. This method of electrostatic stabilization by functional groups is sensitive to pH and different functional groups will stabilize at various pH levels. For example, a number of studies by Daou *et al.* have demonstrated that grafting biphosphonate groups to magnetic nanoparticles at physiological pH values, allows for a higher level of grafting than other functional groups due mainly to the strong P-O-Fe bonds at that pH. Other chemicals reported in the literature that are used to stabilize the surface of SPIONs include tetramethylammonium hydroxide (TMAOH) (Euliss *et al.*, 2003) and Disperbyk 120 (Sen *et al.*, 2006). In general, electrostatic stabilization is a non-covalent process which can pose potential problems for nanoparticles stabilized via this

method when used for *in vivo* applications. A current strategy to improve functional group stabilization is to increase the number of anchoring points on the nanoparticle surface allowing for improved adsorption of the functional groups (Mahmoudi *et al.*, 2010).

1.3.4.c SiO_2 coated SPIONs

Inorganic coatings, such as gold and silica, are also used to electrostatically stabilize magnetic nanoparticles in a colloid. These inorganic materials including metals such as aluminum (Choi *et al.*, 2007) and cadmium, as well as organic dye materials are commonly used for post-synthesis modification of SPIONs which will adopt the core-shell nanoparticle structure. Recently, silica has received a great deal of attention for this purpose. Due to its biocompatibility, low cost, and allowance for covalent stabilization over a broad range of pHs, silica (ie. silicon dioxide) has become an ideal choice for post-synthesis modification of SPIONs to be used for biomedical applications (Alcala *et al.*, 2006) (Ma *et al.*, 2006). Silica is highly suitable for preserving the intrinsic magnetic properties of SPIONs by helping to prevent oxidation and aggregation of the SPION's magnetite core (Bumb *et al.*, 2008). Due to its negative charge, silica has been shown to cause a Coulomb repulsion between the magnetic particles. In addition, depending on the thickness of the silica deposited on the surface of the nanoparticles, the magnetic interaction between the particles can be decreased resulting in fewer agglomerations being formed. Perhaps silica's most significant advantage as a surface coating is that it provides a silanol surface functionality which can facilitate strong covalent coupling processes with alcohols and organosilane coupling agents including many biomolecules and drugs (Liu *et* al., 2004). The attractiveness of organosilanes as coupling agents lays in the extreme diversity of the R group associated with these molecules. This diversity offers the

potential to functionalize and tailor the SPION surface to a wide range of biomedical applications.

Philipse *et al.* in 1994 were the first to report using an amorphous silica coating on a magnetite core using a sol-gel technique. Due to silica's hydrophilic properties, the core-shell nanoparticles were reported to be well distributed in an aqueous solution. More recently in 2004, reverse microemulsion, similar to the method discussed in section 1.3.3, was used by Gupta *et al.* for silica coating SPIONs with coatings as thin as 1 nm being reported.

1.4 Characterization of SPIONs

1.4.1Physical characterization

The magnetic properties of SPIONs depend heavily on their physical characteristics, such as morphology, size, size distribution, crystalline structure, colloidal stability and surface charge. Therefore, characterization of the physical properties of SPIONs is essential in order to properly determine their role in biomedical applications. To date, SPIONs have been widely characterized with respect to these characteristics.

There are a variety of methods available to measure the size, size distribution and morphology of SPIONs in a colloidal suspension or dry state (Mahmoudi *et al.*, 2011). It is generally accepted that the size measurements of SPIONs in suspension are more valuable in consideration of their biomedical applications because the measurements taken in the dry state do not include the salvation shell around the SPIONs that would be observed *in vivo* (Mahmoudi *et al.*, 2011). Moreover, the process of drying SPIONs can affect the aggregation of the nanoparticles and subsequently the cluster or particle size. The most common techniques used in order to determine SPION size include dynamic light scattering (DLS), transmission electron microscopy (TEM), analysis of X-ray diffractograms (XRD) and extended X-ray absorption of fine structure (EXAFS). Scanning electron microscopy (SEM) is also used to characterize the size and morphology of nanoparticle samples (Bumajdad *et al.*, 2011). Atomic force microscopy (AFM) and, by extension, magnetic force microscopy (MFM), are also effective techniques for determining size and size distribution of SPIONs. Of these techniques, DLS is the only technique that determines the nanoparticle size in suspension while the others determine the crystallite size in the dry state. DLS or photonic correlation spectroscopy (PCS) is used to derive the size

distribution of the nanoparticle suspension (Bumajdad *et al.,* 2011). These techniques analyze the sample by measuring the hydrodynamic diameter of the SPIONs in solution. Different from the effective diameter of a particle, the hydrodynamic diameter represents the diameter of a sphere that would diffuse through solution at the same rate as the nanoparticle being measured. Therefore, the hydrodynamic diameter of the nanoparticles is influenced by the mass and shape of the nanoparticles, as well as the ionic force, viscosity and temperature of the solution (Laurent *et al.,* 2010). Dynamic light scattering has a high sensitivity for the presence of agglomerated particles and is able to analyze samples containing a large range of particle sizes and, thus, is particularly useful for studying SPIONs. XRD provides no information on size distribution, but is instead used to determine the crystalline structure of the nanoparticles (Goikolea *et al.,* 2008). Structural analysis of the nanoparticle crystallite can also be done using Mossbauer spectroscopy (Goikolea *et al.,* 2008). Among the techniques that determine crystallite size in the dry state, TEM is by a wide margin the most powerful technique. TEM can provide the user with details on the morphology, size and size distribution of the SPIONs being studied. Perhaps more importantly, TEM can provide insight into the core-shell structure of coated SPIONs, such as SiO_2 SPIONs, due to the difference in electron density of the core and shell materials (Mahmoudi *et al.,* 2011). Electron diffraction patterns of SPION cores and coatings can be obtained to analyze the crystalline structure of the materials. Bumb and colleagues in a 2008 study used TEM to measure the diameter of silica-coated ultra-small SPIONs. The diameter was determined as the mean of three cross-sectional measurements (Bumb *et al.*, 2008). Thickness measurements of the SiO_2 coating were also taken to develop an optimal protocol to produce ultra-thin (2nm) SiO_2 coating on the iron oxide core (Bumb *et al.*, 2008).

In order to properly understand and predict SPION behaviour under physiological conditions, it is necessary to characterize the nanoparticle surface properties. The surface charge of SPIONs contributes in determining the colloidal stability of a suspension of SPIONs and therefore is an important parameter to consider when characterizing SPIONs. Surface charge can be quantitatively measured as an electric potential, zeta potential, in the interfacial double layer on the surface of the SPIONs in suspension (Bumb *et al.*, 2008). Dispersion stability of a suspension of SPIONs is shown by a large zeta potential, either a positive or negative value. Typically, surface charge is characterized by zeta potential analysis with a ZetaMaster and Nanosizer (Bumb *et al.*, 2008). In 1993, Coey *et al.* found that during processes such as endocytosis and phagocytosis, the cellular interactions of the SPIONs were dependent on the surface charge of the nanoparticles.

1.4.2 Magnetic characterization

There are various tools and techniques, besides MFM, that can be used to determine the magnetic properties of SPIONs and magnetic nanoparticles alike. Most commonly, studies which analyze the magnetic nature of SPIONs use a superconducting quantum interference device (SQUID). A SQUID is a highly sensitive magnetometer used to measure extremely weak magnetic fields on the order of 5×10^{-18} Tesla. SQUID analysis is widely used to confirm that the nanoparticles being studied are in fact superparamagnetic. To do this, hysteresis loops are analyzed. Ferromagnetic material differ from superparamagnetic materials in that their magnetic domains, once aligned in the presence of an external magnetic field, do not return to their original state without the expenditure of energy (Bumb *et al.*, 2008). This relationship between applied external magnetic field and magnetic moment traces a hysteresis loop.

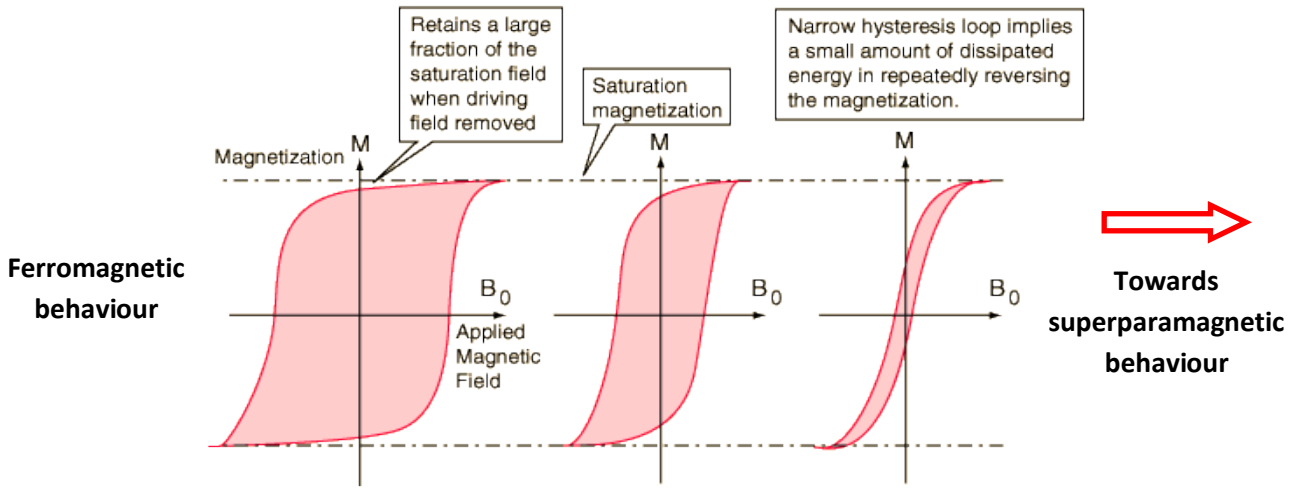

Figure 1.4. Variations in hysteresis curves for different magnetic materials (Nave R., 2009).

In the above figure 1.4, from left to right, the magnetic behaviour becomes increasingly like a superparamagnet. Since true SPIONs do not have a permanent magnetic moment they will have no hysteresis loop. In a study by Schreiber *et al.* in 2008, the superparamagnetic nature of those magnetic nanoparticles being studied was confirmed and demonstrated by showing that the SPIONs could possess a stable dipole moment at room temperature in externally applied magnetic fields on the order of a few hundred gauss (Schreiber *et al.*, 2008).

One can also analyze the magnetic nature of SPIONs using the iron digestion method in conjunction with some basic theory. In 2008, Schreiber *et al.* used the iron digestion method to experimentally determine the concentration of iron in a colloidal solution of SPIONs. As SPIONs are composed of magnetite (Fe_3O_4), and the magnetic moment per Fe_3O_4 molecule is known, the magnetic moment of a small aliquot (50µL) of SPIONs was estimated to be 3.3×10^{-7} Am^2 (Schreiber *et al.*, 2008). With this value, the magnetic moment of an individual SPION can be estimated, but is not considered be highly accurate. Schreiber *et al.* estimated the magnetic

moment of an individual SPION with a 10 nm core to be 2.5 x 10^{-19} Am^2. Both SQUID analysis and the iron digestion method are used to measure mass or aggregated magnetization of colloidal solutions or a small dried mass of SPIONs. Neither is an appropriate technique to measure the magnetic moment of individual SPIONs due to low sensitivity and ultimately poor accuracy. In addition, neither technique measures the magnetic properties of SPIONs in physiologically relevant conditions.

When considering SPIONs it is also important to characterize their magnetic resonance relaxation properties. Relaxometry is used to measure reflexivity or the relaxation variables involved in nuclear magnetic resonance (NMR) and MRI. The relaxation rate of iron oxide nanoparticles is highly dependent on cluster sizes. For example, a cluster of nanoparticles can be considered a superparamagnetic sphere, where all the individual atomic magnetic moments can be treated as a single giant magnetic moment. In this scenario, the transverse relaxation time of the cluster is dependent on the aggregate size and the relaxation rate, R_2, is modified by the state of agglomeration (Laurent *et al.*, 2010). Magnetic properties of SPIONs can be further characterized by using zero field cool (ZFC) and field cool (FC) analyses. These techniques are used to determine the blocking temperature for certain materials which was discussed in section 1.2.2 on superparamagnetism. Mossbauer spectroscopy can also be used for this purpose.

1.4.2.a MFM characterization of SPIONs

Magnetic force microscopy (MFM), a type of scanning probe microscopy associated with AFM, uses a magnetic probe which interacts with the magnetic fields in close proximity to a sample surface. MFM detects local nanoscale magnetic interactions by measuring the magnetic probe deflections caused by the magnetic properties of the surface being characterized. Because

it can image the magnetic field distribution of a sample on the nanoscale and no extensive sample preparation is needed, MFM has proven to be an effective tool for the localization and characterization of micro and macroscale magnetic domains in various materials (Martin *et al.*, 1987 ; Martin *et al.*, 1988 ; Dicarlo *et al.*, 1992). Many studies, both theoretical and experimental have been centred on MFM since it was first developed in 1987 by Martin and Wickramasinghe. These studies include magnetic writing recording media (Qian *et al.*, 1999), magnetic domain wall structures (Zhu *et al.*, 2003), MFM image quantification as well as various simulations and modeling (Gong and Wei, 2007). More recently, MFM has been used to characterize magnetic nanoparticles, mainly ferromagnetic, and has proven itself to be a useful imaging technique for this purpose (Ramlan *et al.*, 2006 ; Takamura *et al.*, 2006) (Pedreschi *et al.*, 2003 ; Park *et al.*, 2008 ; Sievers *et al.*, 2005 ; Puntes *et al.*, 2004). In terms of biological applications, MFM has been used in studying the magnetic properties of biomolecules, magnetotactic bacterium (Proksch *et al.*, 1995) and biogenic nanoparticles (Albrecht *et al.*, 2005). There are iron oxide nanoparticles that naturally occur in biological systems, but there have only been a handful of studies that have reported on the possible use of MFM to detect these particles. These studies include the detection of iron compounds associated with neurological disorders (Dobson, 2001), magnetic domains in magnetotactic bacteria (Diebel *et al.*, 2000) and iron deposits in livers with Hepatitis B (Martinelli *et al.*, 2004).

With respect to characterization to SPIONs, MFM is an underused technique that shows great potential. There are even fewer studies that report on detecting magnetic nanoparticles, specifically SPIONs, *in vitro* (Rasa *et al.*, 2002) or in cell-like systems at ambient conditions (Zhang *et al.*, 2009). A recent study by Schreiber *et al.*, 2008 examined the application of MFM

for the detection and localization of SPIONs. Agglomerations of small SPION (<10 nm) clusters were successfully imaged by MFM for the first time.

2.0 Research Objectives

2.1 Motivations for study

SPIONs are a very important class of magnetic nanoparticles due to the fact that they are magnetized only in the presence of an external magnetic field. As a result, SPIONs are popularly used in a large variety of therapeutic and diagnostic biomedical applications, both *in vitro* and *in vivo*. As a result, they have developed an intimate relationship with cells and other physiological components. In the case of cell separation techniques or hyperthermia treatment, interaction between the SPIONs and cell membrane is adequate. Whereas for drug delivery applications, it is beneficial to have SPIONs enter cells. Thus, for the benefit of biomedical applications of magnetic nanoparticles it is important that the location of the particles can be determined with a degree of high accuracy (Neves *et al.*, 2010). Proper characterization and monitoring of the relationship between cells and SPIONs is central to their potential cellular applications. Currently, one of the most common methods for intracellular imaging of magnetic nanoparticles is fluorescence microscopy. A disadvantage of this technique is that nanoparticles must first be labeled or modified with fluorescent probes in order to be visualized. Furthermore, the maximum resolution of this technique is limited to half the wavelength of the light being used (Bertorelle *et al.*, 2006). In 2010, Sun *et al.* conjugated fluorescent probes to the surface of magnetic nanoparticles in an effort to map cellular uptake pathways. Relative to fluorescence microscopy, two-photon microscopy (TPM) offers improved resolution and has also been used to study cellular interactions with magnetic nanoparticles but still requires the particles to be labeled with a two-photon fluorescent dye (Bergey *et al.*, 2004). Due to the relatively poor resolution and reliability of these techniques, a label-free *in vitro* detection method for magnetic nanoparticles,

SPIONs especially, is of great interest. Magnetic force microscopy (MFM), because of its ability to localize, characterize and distinguish magnetic nanoparticles from other particles at the nanoscale without labeling, as well as the three-dimensional nature of the information it provides, fits these needs and offers great potential for this purpose.

MFM has the capability to detect nanoscale magnetic domains, such as magnetic nanoparticles, as well as simultaneously obtain both atomic force microscopy phase and topography images. Yet, this technique has received limited attention as a potential tool for characterization of SPIONs, specifically in physiologically relevant conditions. The majority of studies that have used MFM to characterize SPIONs or other magnetic nanoparticles have done so under ambient conditions (Schreiber *et al.*, 2008; Rasa *et al.*, 2002; Zhang *et al.*, 2009). SPIONs, however, carry out their function in physiological conditions. Therefore, characterization of these particles should be undertaken in conditions similar and relevant to the physiological environment. The potential of MFM is largely unexplored in this regard.

In this study, we attempt to investigate the capability of MFM to detect and characterize SPIONs covered by multilayer phospholipid membranes in both air and liquid. The end goal of this study is to evaluate the ability of MFM to detect the magnetic signal of SPIONs under the influence of an external magnetic field in physiologically relevant conditions (ie. fluid environment with lipid membranes). Such research is vital to future applications of MFM, including the potential to image magnetic nanoparticles unlabelled and unmodified in living cells.

2.2 Rationale for experiments

Magnetic signal strength for both bare and silica-coated SPIONs will be measured and characterized MFM. Data will be analyzed to determine if any variation in magnetic signal strength exists between bare and silica-coated SPIONs. A 2008 study by Bumb *et al*. using SQUID magnetometry suggested that under low applied magnetic fields, SiO_2 coated SPIONs have a larger magnetic moment than bare SPIONs. We want to investigate this effect on the nanoscale by imaging individual SPIONs instead of large batch analysis like those used with SQUID magnetometry. Variation of the magnetic moment of a SPION due to the presence of a surface coating (ie. silica) may influence how controllable the nanoparticles will be when used for biomedical applications such as targeted drug delivery and therefore is an important characteristic to consider when magnetically characterizing SPIONs.

As mentioned in section 2.0, the end goal of this study is to use MFM to magnetically characterize SPIONs in physiologically relevant conditions covered with synthetic membrane phospholipids. This requires that the SPIONs be imaged in an aqueous environment. To avoid removing the SPIONs from the surface of the substrate, it is necessary that they are fixed to the mica before being introduced into the aqueous environment and subsequently covered with synthetic membrane phospholipids. My goal was to develop a sample preparation protocol for the deposition of SPIONs such that liquid can be introduced during imaging without removing the particles from the surface of the substrate. To this end, several approaches were explored.

Poly-L-lysine (PLL) was used first in this study, primarily due to its immediate availability, in an attempt to adhere the SPIONs to the mica surface. PLL is a synthetic, positively charged amino acid. It is commonly used to coat silicon-based substrates to provide and enhance attachment and adhesion of cells and other biological entities relying on the

negative charge of phospholipid membranes. Moreover, the covalent attachment of synthetic amino acids, like PLL, to silica nanoparticles is well established. In 2010, Kar *et al*. covalently attached PLL to silica nanoparticles in order to impart the silica nanoparticle's surface with a high level of cationic charges. For these reasons, PLL was investigated as a potential tool to link the SiO_2 SPIONs to the slightly negatively charged mica.

As a preliminary objective to covering SPIONs with synthetic phospholipid membranes, several methods were also explored using various materials as analogues for lipid bilayers to cover the SPIONs on the mica in addition to securing them to the surface of the substrate. Hydrophobic polymers poly (methyl methacrylate) (PMMA) and polystyrene (PS) were used to spin-coat SPION samples prepared on mica. Agarose and polyacrylamide were also investigated as potential media to coat or embed the SPIONs on the mica substrate. These hydrophobic polymers served as an analogue for a lipid bilayer in that they created a hydrophobic coating over the SPIONs with thickness comparable to a phospholipid bilayer. Coating the sample with a PS or PMMA will secure the nanoparticles to the substrate and prevent the SPIONs from being removed from the substrate when they are exposed to water. Therefore, the spin-coated polymer will allow the SPIONs to be imaged in both air and liquid environments. MFM could then be used to map the magnetic signal of the SPIONs from underneath the hydrophobic polymer in relation to hover mode scanning height from the sample. Variation in hover mode scanning height is necessary to mimic the distances that could be encountered if the SPIONs were to be imaged from within a cell and to determine the distance at which the magnetic signal from the SPIONs has diminished to the point that it can no longer be detected.

The last method investigated which used an analogue for a lipid bilayer to cover the SPIONs on the mica involved the use of tetraethylorthosilicate (TEOS). TEOS is a chemical

compound mainly used as a crosslinking agent for silicone polymers. TEOS has the unique property of being easily converted to silica (SiO_2). This reaction takes place upon the addition of water and converts the TEOS molecule into a translucent solid with a mineral-like structure comprised of Si-O-Si bonds. A 2009 study by Roiter *et al.* used TEOS to provide fixation of silica nanoparticles to silicon wafer substrates. Samples of silica nanoparticles already deposited on silicon wafers were treated with TEOS and then kept in buffer in order to hydrolyze the TEOS consequently forming a thin layer of silica helping to secure the silica nanoparticles to the surface of the sample.

Due to the limited success of the techniques mentioned thus far, we decided to pursue chemical means of adhering the SPIONs to the surface of the substrate (ie. formation of a covalent bond between the SiO_2 SPIONs and the substrate) rather than physical means. The most promising method attempted to date for securing the SiO_2 coated SPIONs to the mica is the use of gold-coated mica substrates further modified with 3-mercaptopropyltrimethoxysilane (3-MPTS), an organosilane. The key to this method is the formation of a covalent bond between the gold coated substrate and the SiO_2 coated SPION via the 3-MPTS molecule, specifically via its thiol functional group. Formation of this covalent bond will provide stability in air and liquid environments. An illustration of this deposition method as well as the chemical structure of 3-MPTS is shown in the following figure 1.5.

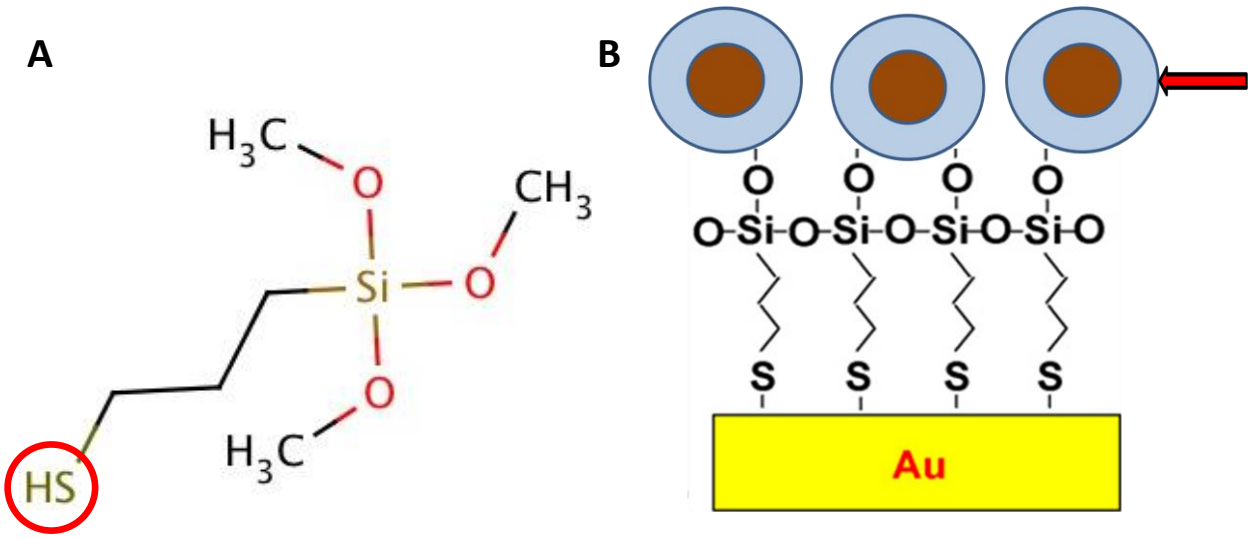

Figure 2.1. Deposition of SiO_2 coated SPIONs via (3-MPTS). A) Chemical structure of 3-MPTS with the red circle indicating the thiol functional group. B) Illustration of SiO_2 deposition with the red arrow indicating the SiO_2 coating containing the silanol functional group.

After the SPIONs were secured to the surface of the mica via 3-MPTS, samples could then be coated with lipid membranes in a liquid environment. The chemistry involved in thiol-gold interactions is well established and documented making this an attractive method. Moreover, this technique was used by Vakarelski *et al*. in 2007 in order to immobilize SiO_2 nanobeads on gold coated silicon wafers demonstrating its potential for the purposes of this study.

The end goal of this study is to use MFM to magnetically characterize SPIONs in physiologically relevant conditions covered with synthetic membrane phospholipids. This will allow us to understand the feasibility of detecting magnetic nanoparticles within cell membranes without any labeling or modifications and evaluate MFM as a potential magnetic analogue for fluorescence microscopy. We hope by showing that SPIONs can be imaged with MFM when covered with phospholipid membranes, that a more accurate and detailed understanding of the characteristics of SPIONs and magnetic nanoparticles in biological systems can be gained. These

results could potentially lead to cell studies and a better understanding of how SPIONs distribute themselves inside the cell and ultimately have a valuable impact for biomedical applications of all types of magnetic nanoparticles.

3.0 Materials and Methods

3.1 Atomic force microscopy

Atomic force microscopy (AFM) is a type of scanning probe microscopy (SPM) that allows topographical imaging of surfaces at nanoscale and even atomic resolution. AFM uses a Raster scanning system with two scans per line, a trace and a retrace. AFM utilizes a cantilever with a sharpened probe to physically scan the surface of the sample being imaged in one of two modes: either 'contact' or 'tapping' (intermittent contact). When the probe comes into contact with the surface it is influenced by various attractive or repulsive atomic forces (Van der Waals forces, coulombic forces etc). As the cantilever interacts with the surface, it is deflected by these atomic forces. A laser beam reflected off of the cantilever onto a photodetector detects the fine movements of the cantilever. The movement of the laser on the photodetector is processed by an electronic feedback system and allows for a detailed 3D image of the surface to be produced and displayed on the computer screen. Depending on the mode of AFM being used, the electronic feedback system will attempt to keep constant either the force of the probe on the specimen (contact mode) or the amplitude of the cantilever oscillations (intermittent contact mode). Any variations from these constants is processed by the electronic feedback system and used to create an image. AFM is a very valuable technique as it can achieve atomic scale resolution, and can perform scans in both liquid and air. AFM also requires relatively easy sample preparation when compared to other imaging techniques such as TEM, in particular when it comes to imaging biological samples. The schematic shown in figure 3 A) illustrates how cantilever deflections are detected as the tip scans the surface of a sample.

3.2 Magnetic force microscopy

Magnetic force microscopy (MFM), a type of scanning probe microscopy associated with AFM, uses a magnetic probe which interacts with the magnetic fields in close proximity to a sample surface. MFM detects local nanoscale magnetic interactions by measuring the magnetic probe deflections caused by the magnetic properties of the surface being characterized. In oscillating lift mode MFM as used here, the image contrast is formed by the change in effective spring constant of the cantilever caused by the interaction between the magnetic fields above the SPIONs with the field from the probe. This causes a shift in the frequency of oscillation which is most commonly detected by the effect it has on the phase of oscillation of the waveform that models the oscillating cantilever (Neves *et al.,* 2010). The phase shift detected by MFM is measured in degrees and represents the phase difference between the oscillation of the cantilever before and after encountering a magnetic field. The original waveform, before having encountered a magnetic field, will now be offset either right (positive phase shift) or left (negative phase shift).

MFM is a very useful method because it is able to detect the magnetic field above the sample surface in addition to providing an AFM topography image. MFM accomplishes this by using the 'hover mode' scanning method and an AFM probe with a magnetic coating. This is the most commonly used method for MFM, because it is relatively simple to implement and commonly will provide high phase contrast in ambient conditions (Neves *et al.*, 2010). On the first trace of the sample, the cantilever directly scans the surface of the sample just as it would for AFM in intermittent contact mode. Subsequently on the retrace, the cantilever is raised to a user defined height (eg. 50 nm) away from the surface and scans for the magnetic signal by following the topographical pattern from the previous trace as seen in figure 3.1 B). On the first

trace, short range interactions (ie. Van der Waals forces) have the most significant effect on the cantilever, and subsequently, MFM delivers a topography image just as with AFM. On the hover mode retrace, long range interactions such as magnetic forces are most prevalent, therefore on the second trace, the MFM image will reflect the magnetic properties of the sample. During the initial trace, it is possible that samples are magnetized. Consequently, it is inherent in lift mode MFM that the cantilever tip will often magnetize very small magnetic domains.

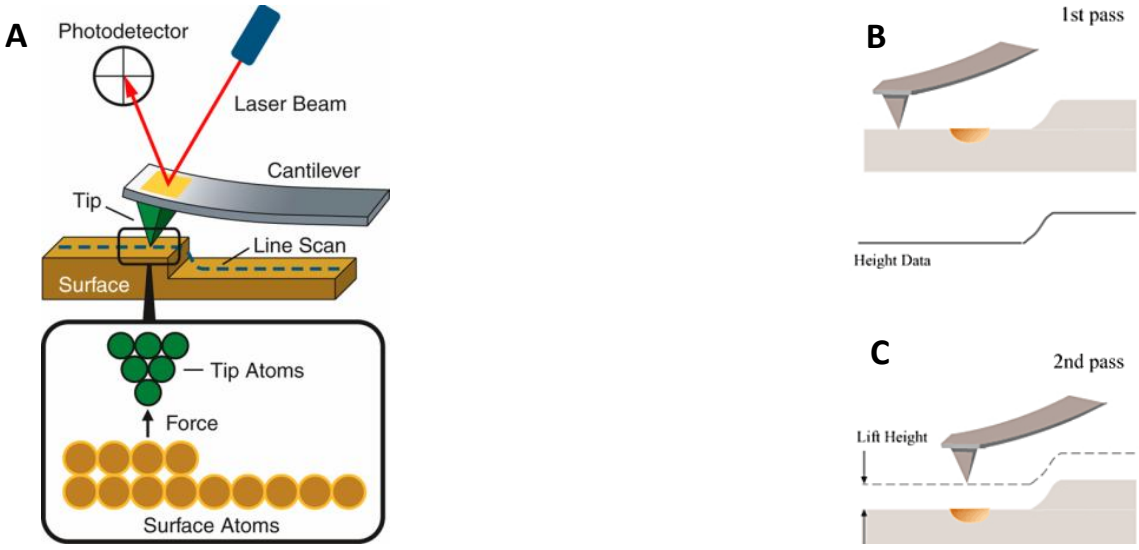

Figure 3.1. Schematic of AFM and MFM imaging techniques. A) An AFM tip scans the surface of a sample and a laser reflected off of the cantilever onto a photodetector measures any cantilever deflection. B and C show a schematic of MFM hover mode scanning method. In B) the tip scans the surface of the sample just as it would with AFM. Panel C) shows the retrace where the cantilever is raised to a user defined height away from the surface. The cantilever then follows the identical topographical pattern and scans for the magnetic signal of the sample. (www.nano.tm.agilent.com/measurementsinnanotechnology)

3.3 Experimental section

3.3.1 SPION synthesis

Materials

Iron (II) chloride (99%, Sigma), iron (III) chloride (99%, Sigma), tetramethylammonium hydroxide (TMAOH) (25% solution, Sigma), tetraethyl orthosilicate (TEOS) (99%, Sigma), ammonium hydroxide (28% solution, Sigma), and ethanol (99%, ACS) were purchased and used without further purification.

SPION synthesis

Bare and SiO_2 coated SPIONs were synthesized by a co-precipitation method at the University of Waterloo in Dr. Frank Gu's Lab. 2.5 mL of a mixed iron solution in deionized water (2 mol/L $FeCl_2$ and 1 mol/L $FeCl_3$) was added to a 0.7 mol/L tetramethylammonium hydroxide (TMAOH) solution under vigorous stirring, and the reaction was allowed to proceed open to the air at room temperature for 30 min while stirring. After 30 min, the black particles were separated from solution over a neodymium magnet, and washed at least thrice with an equivalent volume of pH 12 TMAOH solution (so as to maintain the equivalent particle concentration as immediately after the reaction), until the particles were no longer magnetically separable. The effect of TMAOH on the SPIONs in solution will be demonstrated and addressed in the results and discussion section of this thesis. This colloidal suspension was sonicated for 10 min (Branson Digital Sonifier 450, USA), and then 20 mL of the sonicated fluid was mixed with 20 mL pH 12 TMAOH and 160 mL ethanol. 7 mL tetraethylorthosilicate (TEOS) was then added to this suspension while stirring, and allowed to react at room temperature while stirring for ~18 h. The SiO_2 coated SPIONs were then magnetically recovered from solution, and washed thrice

with ethanol and thrice with deionized water by magnetic decantation, and sonicated into deionized water for 10 min before further use.

3.3.2 SPION deposition on bare mica

A SPION dilution of ~5.5 mg/mL was prepared using Millipore water. A concentration of ~5.5 mg/mL of SPIONs was used because it was observed to provide a uniform distribution of SPIONs with a relatively small size distribution where individual particles could be observed. The SPION dilution was sonicated for 30 minutes before being deposited on mica. 10µL of the SPION dilution was deposited on freshly cleaved mica (v-4 grade, SPI Supplies, PA, USA), covered and let air dry for ~ 6 minutes. The sample was rinsed with ~ 4 – 5 drops of Millipore water and then immediately dried with a steady stream of nitrogen for 3.5 minutes. Finished samples were placed in a sealed petri dish with nitrogen and left in a dessicator overnight.

3.3.3 PS and PMMA coated sample preparation

The same protocol covered in section 3.3.2 was followed in order to prepare the SPION samples on mica before being coated with polymer. Either a 3% solution of PMMA or a 0.4% solution of PS was used to spin coat the SPION samples with a coating of ~ 30 nm. Both PMMA and PS dilutions were made in toluene. 40µL aliquots of the respective polymer solutions were pipette onto the already prepared SPION samples. A spin motor with an applied voltage of 1V for 15 seconds was used in order to spin coat both the PMMA and PS. The voltage applied to the motor is proportional to the thickness of the spin-coated polymer. The same imaging protocol (to

be covered in section 3.3.6) was used to image the SPION samples prepared with PMMA or PS coatings.

3.3.4 Substrate (mica) modification via TEOS

Silicon wafers were sonicated in absolute ethanol for 15 minutes, then immediately sonicated in methylene chloride for 30 minutes. The silicon wafers were then thoroughly rinsed with water and dried with a steady stream of nitrogen. Once they were dry, the silicon wafers were placed in a UV cleaner for 1 hour. All silicon wafers were pre-treated with TEOS before use. To pre-treat the substrates with TEOS, vapour deposition was used. A paper filter was placed inside a petri-dish and soaked with 20µL of TEOS then silicon substrates were placed inside the petri-dish, covered with a lid, and incubated for 2 hours at 50°C. Cast deposition was used to deposit 10µL of an approximately 5.5mg/mL solution of SPIONs in water. SPION solutions were sonicated for 30 minutes before being deposited on the silicon surface.

3.3.5 Substrate (mica) modification via 3-MPTS

Circular mica substrates were freshly cleaved and stored in nitrogen. The mica substrates were then sputtered with a 2.5 nm layer of titanium using an electron bean evaporator. Subsequently, a 50 nm layer of gold was deposited onto the titanium layer without interruption of the vacuum ensuring that titanium dioxide did not form on the surface of the substrate. After sputtering, mica substrates were stored in nitrogen until needed. Sputtered gold wafers were immersed in a 40mM solution of 3-MPTS in methanol for 3 hours. Substrates were then

thoroughly rinsed with methanol and Millipore water. After immersion in methanol, substrates were then placed into an aqueous 0.01 M NaOH solution for 1 hour. Substrates were then immersed in a solution of SiO_2 SPIONs (~6.9mg/mL) for 1 hour. To finish, substrates were washed with Millipore water and dried with nitrogen gas. Samples were imaged immediately.

Unfortunately, the study never reached this stage due to availability of materials but the details for deposition of lipid membranes are as follows. Lipid preparation will be done using the dry method of vesicle fusion as shown by Leonenko et al. in 2000. Using this method, dioleyl phosphatidyl choline (DOPC) vesicles will be made at a concentration of 0.5mg/mL. Powdered DOPC will be suspended in nanopure water to a concentration of 0.5mg/mL. In order to create a lipid solution with uniform sized vesicles, the solution will be sonicated for 10 minute intervals between which the lipid solution will be stirred at room temperature for 15 minutes. After the solution has become clear and uniform vesicles are present, it will be filtered using 0.2µm filter caps on syringes.

AFM and MFM imaging in liquid will be done in the JPK liquid cell. The SPIONs will first be imaged in approximately 50µL of Tris-HCl buffer. Next, the buffer will be carefully removed and replaced with 5-20µL of DOPC lipid suspension. Images will be taken periodically to provide a picture of the lipid bilayer formation on the SPIONs without being disturbed by the MFM tip. All imaging will be done with intermittent contact mode in fluid, using the same cantilever and external magnetic field.

3.3.6 MFM imaging

All samples were imaged using a JPK atomic force microscope (JPK Instruments, Germany). MikroMasch NSC-18, cobalt/chromium coated magnetic cantilevers (MIKROMASCH USA, CA, USA) were used to image the SPIONs. An external perpendicular magnetic field (relative to the measurement direction) was applied to the sample during imaging in order to ensure magnetization of the SPIONs and to improve and heighten the contrast of MFM phase images. The external perpendicular magnetic field was applied to the sample by placing a small permanent magnet directly underneath the mica during imaging. All samples were imaged using intermittent contact mode with hover mode.

4.0 Results and Discussion

4.1 Methods for securing SPIONs to substrate in liquid

As mentioned in section 2.1, to avoid removing the SPIONs from the surface of the substrate during MFM imaging in liquid, it is necessary that they are fixed to the mica before being introduced into an aqueous environment. In order to achieve this, I wanted to develop a protocol for the deposition of SPIONs such that water can be added to the sample during liquid imaging without disturbing the nanoparticles. The results of unsuccessful approaches are mentioned briefly in this section. Further discussion and results for successful methods will be addressed in the following sections.

Briefly touched upon in section 2.1, PLL was investigated first as a potential tool to link the SiO_2 SPIONs to the slightly negatively charged mica due to PLL's positive charge and ability to covalently attach to silica nanoparticles as shown by Kar *et al* in 2010. Unfortunately for this thesis, when the PLL samples were imaged using MFM, extremely rough surfaces with large globular structures (~200 nm) were observed suggesting that very large aggregations of SPIONs had formed with PLL that are unsuitable for the purposes of this study. The following figure 4.1 displays an AFM image of these large aggregations.

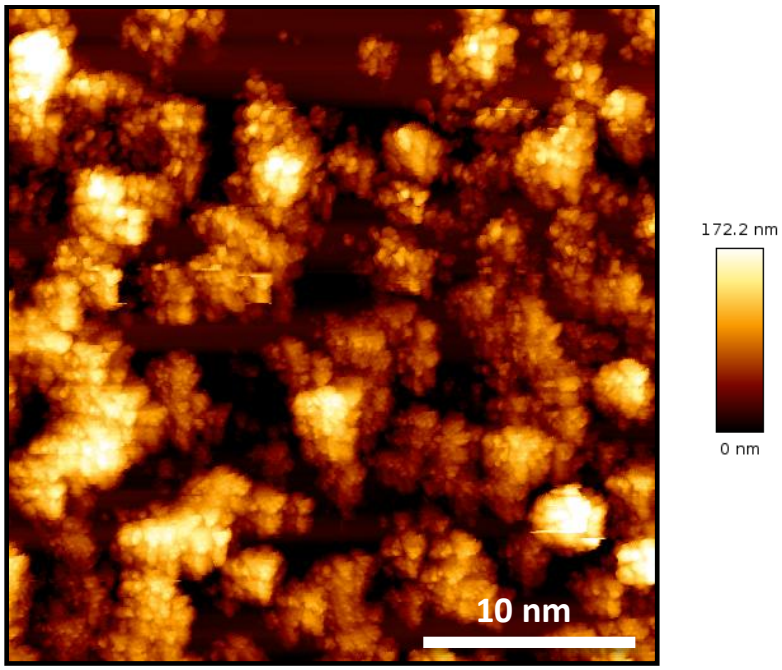

Figure 4.1. AFM topography image of SPIONs with PLL on mica. Images were taken using a magnetic AFM probe in the presence of an externally applied perpendicular magnetic field in ambient conditions. Colour-scale is shown to the right of the image and scale bar is located in the bottom right of the panel.

These approximately 200 nm sized agglomerations are not suitable for MFM because of the sharp peaks possessed by these structures. Although MFM is capable of imaging samples with varying non-flat topographies, samples with large drastic "peaks and drops," like those seen in figure 4.1 can cause the MFM cantilever to "crash" into the surface of the sample producing false MFM signals and ultimately inaccurate results. For these reasons, this technique was unreliable and thus discontinued.

Agarose and polyacrylamide were also investigated as potential media to coat or embed the SPIONs on the mica substrate. Although initially promising, methods involving these materials were met with difficulty during the imaging process. Both substrates, due to a low coefficient of static friction, caused the cantilever to 'skip' along the surface of the sample,

producing no useable images and making imaging the sample very difficult and ultimately not practical for this MFM technique.

4.2 Bare vs. SiO_2 coated SPIONs

In order to compare the magnetic properties of bare and SiO_2 SPIONs at the nanoscale, MFM analysis was performed on samples of each type of SPION deposited on mica as described in section 3.3.2. Figure 4.2, panels A through D, show the AFM and MFM phase images used for comparison of the bare and SiO_2 coated SPIONs. AFM topography images (panels A and C) were used to construct the size distributions for both types of SPIONs seen in figure 4.2 panels F and G. Both SPIONs were found to have non-symmetric right skewed size distributions with the SiO_2 SPIONs having a broader distribution and a higher mean diameter (measured using the z height detected by the cantilever) than the bare SPIONs. This observation is supported by TEM analysis seen in figure 4.2, panel E. The TEM analysis suggests that a non-uniform coating of silica forms around and between individual particles, subsequently forming larger aggregates. The mean, median and mode diameter measured for bare and SiO_2 coated SPIONs were 5.1 +/- 0.1nm (standard error), 4.0 nm, 1.2 nm and 33 +/- 1 nm (standard error), 13 nm, 4 nm respectively. Although MFM detection of SPIONs has been reported, there is some doubt whether individual SPIONs can actually be distinguished by MFM because the magnetic field from SPIONs is proportional to the diameter of the particle and thus very small. In 2009, silica nanoparticles, with and without the presence of a magnetic core were compared using MFM (Pacifico *et al.* 2009). When the magnetic core was absent, no MFM contrast was observed suggesting that only magnetic structures will cause measurable phase contrast. In figure 4.2, MFM contrast is observed for SPIONs as small as ~ 3nm. As a result, we can be confident that these are true MFM signals from the SPIONs being studied.

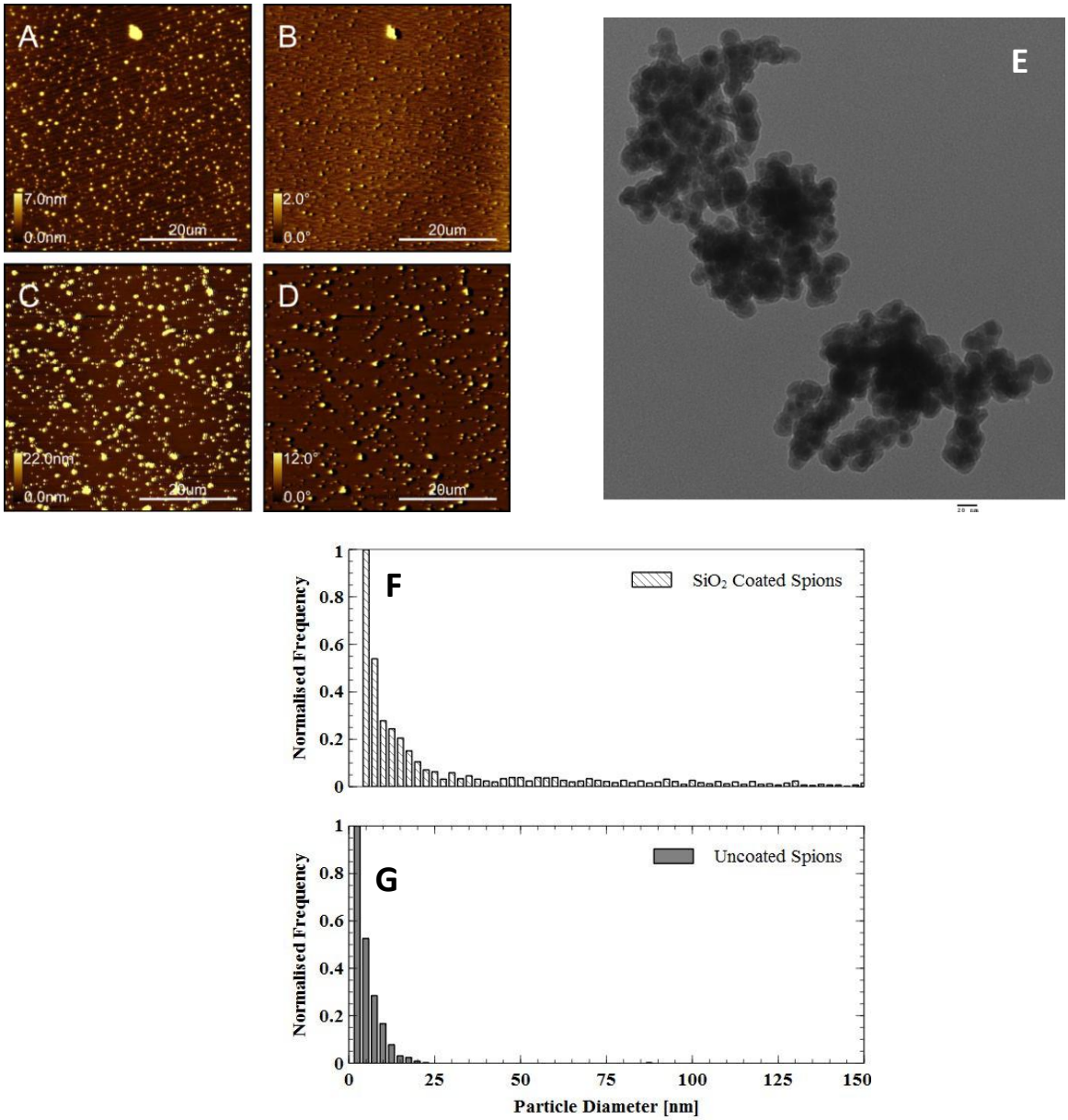

Figure 4.2. Characterization of bare vs. SiO_2 coated SPIONs. A-D) Tapping-mode AFM topography images (column 1) and MFM phase images (column 2) of bare and SiO_2 coated SPIONs (images A/B and C/D respectively). Both topography and MFM phase images obtained using a magnetic AFM probe in the presence of an externally applied perpendicular magnetic field in ambient conditions. MFM phase images obtained in lift mode at a scan height of 50 nm. Colour-scale and scale bars for both topography and phase images are shown in the bottom of each panel. E) TEM image (taken by Frank Gu Research Group) of SiO_2 coated SPIONs demonstrating that the majority of the SiO_2 coated SPIONs are agglomerations of small particles. Dark gray areas representing the SPION magnetite core and the lighter gray regions are the silica coating. Scale bar is shown in the bottom right of panel. F/G) Size distributions for both bare (F) and SiO_2 coated (G) SPIONs.

In oscillating hover mode MFM, as used in this thesis, the contrast observed in the MFM images is caused by the interaction between the magnetic field from the sample (including external perpendicular magnetic field) and the field from the MFM probe. These interactions cause a shift in the frequency of the oscillating probe of the cantilever which manifests itself as an effect on the phase of the oscillation (Hartmann, 1999 ; Belliard, 1997). The MFM images for both types of SPIONs shown Figure 4.2, panels B and D demonstrate an effect called dipolar contrast, with half of the phase contrast being dark, and half being light for each individual magnetic structure. This dipolar contrast for magnetic nanoparticles is typically found only when external magnetic fields are applied perpendicularly to the measurement direction (Schreiber *et al.*, 2008 ; Pacifico *et al.*, 2009 ; Mironov *et al.*, 2007) (Neves *et al.*, 2010) as is the case for this thesis.

In order to directly compare the magnetic properties of individual bare and SiO_2 coated SPIONs, the MFM phase-shift for each bare and SiO_2 SPION, gathered from the MFM phase images (figure 4.2 panels B and D) was plotted as a function of particle size (diameter) in figure 4.3. A positive linear trend is observed for both types of SPIONs. This data suggests that the magnetic moment is proportional to the diameter and therefore the volume of the SPION. Computer simulations of MFM on SPIONs have also demonstrated that the phase shift detected in MFM depends very strongly on the particle diameter (Mironov *et al.*, 2007). A 2008 study by Bumb *et al.*, noted that under low applied fields, higher magnetization values were observed for silica-coated SPION samples when compared to uncoated SPIONs; suggesting that silica separating the small particles may be leading to weak ferromagnetic ordering in the relatively large batches of nanoparticles that are required for SQUID analysis. We found bare and SiO_2 coated SPIONs are shown to behave identically when analyzed with MFM, demonstrating that

the SiO_2 coating has no effect on the magnetic properties of the SPIONs, contrary to large batch analysis using SQUID. A similar result was also observed by Neves *et al.* in 2010 which found that the response of MFM to magnetic nanoparticles is not affected by the presence of a silica coating.

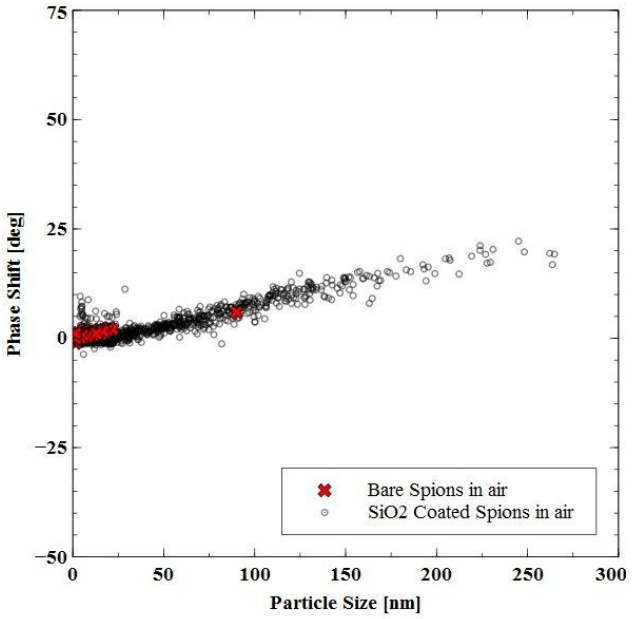

Figure 4.3. MFM phase-shift vs. particle size for bare and SiO_2 coated SPIONs. Phase-shift values obtained in MFM experiments on bare and SiO_2 coated SPIONs described in Figure 4.2. Phase shift (measured in degrees) versus SPION size (nanometers) is shown. A positive linear trend is observed for both bare and SiO_2 SPIONs. Phase shift values for bare SPIONs range from 0 to ~4 degrees and from 0 to ~ 20 degrees for SiO_2 coated SPIONs. MFM analysis for this data set was done in ambient conditions.

4.3 MFM phase-shift dependence on scan height

To understand the limits to the detection of small SPIONs with MFM, we experimentally analyzed the magnetic force sensitivity of our MFM technique by examining the relationship between MFM phase-shift from SPIONs and hover mode scan height as described in figure 4.4. To mimic various biological media or membranes which could embed or cover the SPIONs in a physiological system, as well as secure the SPIONs to the surface of the substrate, an approximately 30 nm layer of PS was spin-coated over the SPIONs on mica. From figure 4.4A, the phase contrast in the MFM images is observed to increase with scan height. This relationship can be seen plotted in figure 4.4 C. The data suggests that for this height range as scan height increases, MFM phase-shift measured will also increase reaching a plateau at approximately 300nm.

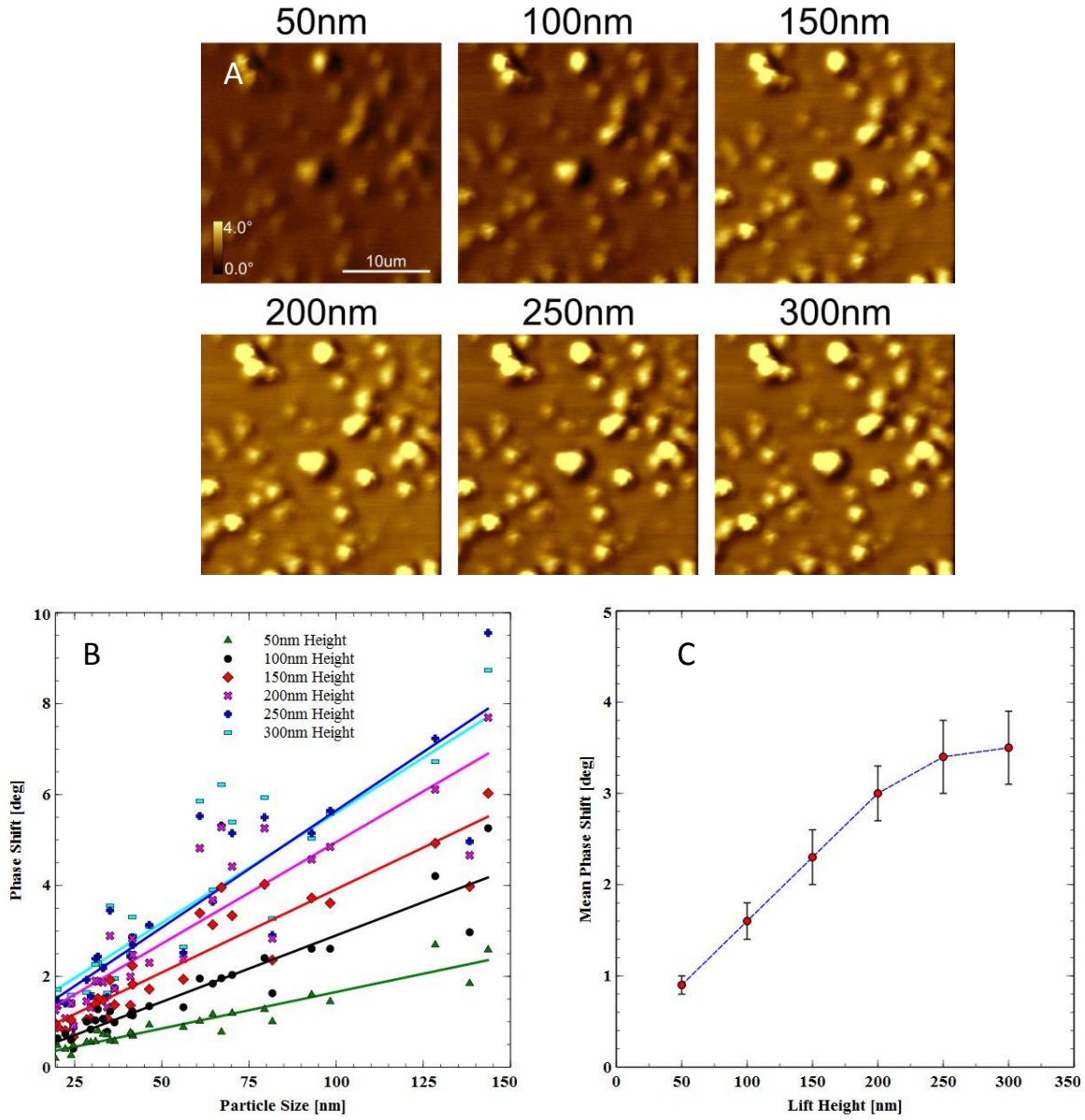

Figure 4.4. MFM phase-shift vs. lift height data for SiO_2 coated SPIONs covered with PS. A) MFM phase images of SiO_2 coated SPIONs spin-coated with PS taken consecutively at lift heights from 50-300nm at 50nm increments. Images were taken using a magnetic AFM probe in the presence of an externally applied perpendicular magnetic field in ambient conditions. Colour-scale and scale bars are shown in the in the 50nm panel (panel 1) and apply to all images in panel A. The magnitude of the MFM phase shift was observed to be largest at the highest scan height of 300nm. B) MFM phase-shift (degrees) versus particle size (nm) is shown for each scan height of SiO_2 SPIONs covered with PS as seen in A. Best fit lines show positive linear trends for these data sets. C) Mean phase shift (for each set of SPIONs of different sizes) versus MFM scan height values for the phase images shown A). An increase in mean phase shift as scan height increases is observed reaching a plateau at 300nm.

Assuming MFM phase-shift measured is proportional to SPION magnetic moment, this result seems counter-intuitive. Consider a situation where only a permanent magnet was being imaged using MFM. One could assume that the same relationship plotted would display MFM phase-shift decreasing as the lift height (z) increases, eventually reaching zero as the lift height approaches infinity. First, the fact that this relationship is not observed in figure 4.4C suggests that the phase-shift being measured is genuinely due to the SPIONs . Yet, the fact that the phase is increasing with lift height is problematic. To explain this, we need to examine an ideal situation in which the MFM probe should be experiencing no magnetic field when the lift height is at infinity (ie. the curve has reached a plateau). Therefore, from a practical point of view, any phase-shift observed at the maximum height of 300nm when the curve plateaus, as seen in figure 4.4C, can be assumed to be a background artefact from the MFM imaging technique and thus should be subtracted from each data point within the curve. The adjusted curve would have been decreased at each data point by the maximum phase-shift value observed at the plateau of the original curve and as a result would plateau just beneath zero. With respect to the adjusted curve; a similar result was reported in a 2010 study by Neves *et al*., which found relative MFM-phase shift to increase with scan height and plateau at approximately 250 nm with the phase-shift approaching zero.

The specific reasons for the cause of this background effect are beyond the purposes and scope of this study. But, it is important to note that magnetic fields being experienced by the MFM probe are non-uniform, and that the phase-shift being measured can be influenced by the specific probe being used. The magnetic field from these probes has been shown to be somewhat non-uniform and vary from probe to probe. This inherent property of a batch of cantilevers can cause misrepresentations and inconsistencies in the measurements of sample magnetic fields

despite using probes from the same batch and magnetizing them with the same method, as done in this thesis study (Schwarz and Wiesendanger, 2008). As demonstrated by Yacoot and Koenders 2008, a series of complicated steps are required in order to take the variability of MFM probes into account. Thus, for the purposes of this study, this variable is unknown and is one of the most significant limiting factors for quantitative MFM (Schaffer *et al.*, 2003).

4.4 MFM of SPIONs in liquid

Although MFM imaging of SiO_2 coated magnetic particles has been shown before (Neves *et al.*, 2010; Pacifico *et al.*, 2009), in this work, we present images of SPIONs that have been coated with analogues for synthetic lipid membranes and imaged using MFM in liquid for the first time. This step served as a proof of principle for using MFM in a liquid environment to magnetically characterize SPIONs. This experiment is also an appropriate preliminary step before using lipid membranes to cover the SPIONs. SPIONs were coated with PMMA according to the protocol outlined in section 3.3.3. Coating the sample with PMMA temporarily secured the nanoparticles to the substrate and prevented the SPIONs from being removed from the substrate when they were exposed to water.

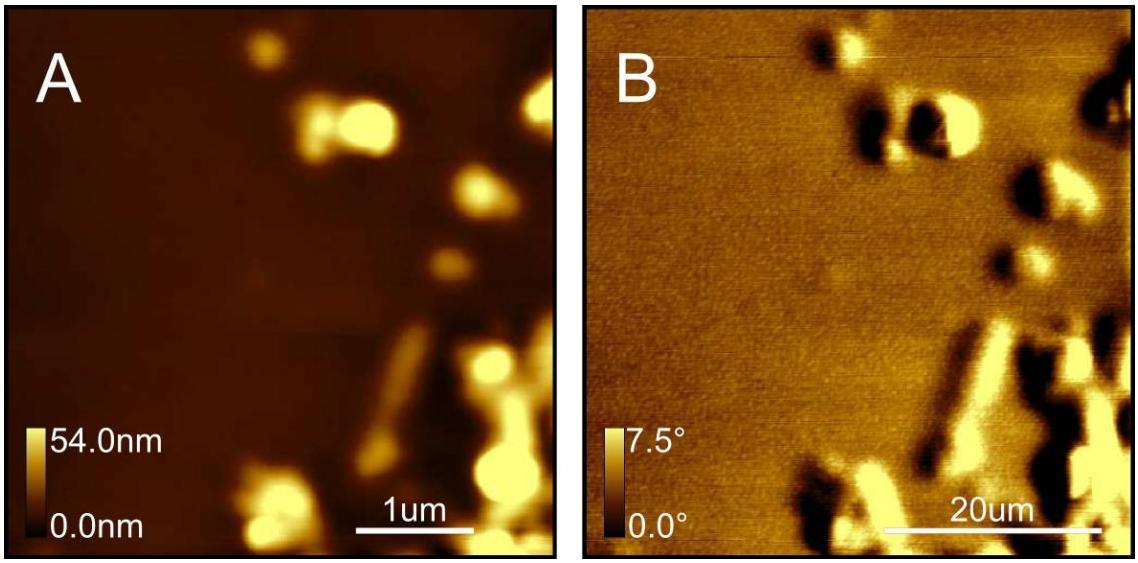

Figure 4.5. MFM in liquid image of SiO_2 coated SPIONs spin-coated with PMMA. Tapping-mode AFM topography image (A) and MFM phase image (B) of SiO_2 coated SPIONs spin-coated with PMMA taken at a lift height of 50nm. Images were taken using a magnetic AFM probe in the presence of an externally applied perpendicular magnetic field in liquid (water). A spin motor with an applied voltage of 1V for 15 seconds was used to spin coat a 3% solution of PMMA (in toluene) in order to cover the SPION sample with ~ 30nm of PS. Colour-scale and scale bars are shown in the in the bottom of each panel.

Relatively small agglomerations of SPIONs covered with an approximately 30 nm layer of PMMA are observed in figure 4.5. Considerably wider more gradual structures are observed in when compared to the SPION structures seen in figure 4.2. This comparison suggests that the SPIONs in figure 4.5 are indeed coated with PMMA. In the MFM image, figure 4.5 panel B, the same dipolar contrast observed in figure 4.2 (panels B and D) can be seen, again due to the external perpendicular magnetic field being applied to the sample.

The SPIONs are shown to cluster in the bottom right hand corner of the image. Although the SPIONs were temporarily secured to the substrate in liquid by the PMMA coating, unfortunately over time, water was allowed to seep between the mica and the PMMA coating, removing the PMMA and causing the SPIONs to slowly migrate on the sample under the influence of the external magnetic field. As a result, the images in figure 4.5 are unfortunately the only images of MFM in liquid presented in this thesis. Even so, when comparing the phase-shift values of the PMMA covered SiO_2 coated SPIONs in figure 4.5B to those SPIONs in figure 4.2D the maximum phase-shift observed for each image is 7 degrees and 12 degrees respectively. Considering that these images were taken with the same batch of SPIONs using the same technique and at the same lift height, one could assume that any difference in phase-contrast between these two samples can be attributed to the PMMA coating. Since only one image of MFM in liquid is presented, further study is required to properly investigate the effect of this hydrophobic coating on MFM phase-shift.

4.5 SPIONs on gold coated 3-MPTS functionalized mica

At this point, chemical means of adhering the SPIONs to the surface of the substrate (ie. the formation of a covalent bond between the SiO_2 SPIONs and the substrate) were considered. For the reasons mentioned in section 2.1, 3-MPTS was investigated for this purpose. SiO_2 coated SPIONs are attached to gold coated mica substrates further modified with 3-MPTS as outlined in section 3.3.5. Although only briefly attempted due to availability of materials, this method is the most promising method attempted thus far for securing the SiO_2 coated SPIONs to the mica.

From the MFM phase image shown in figure 4.6 B, a higher degree of phase contrast from the SPIONs can be observed when compared to figure 4.2 D. Individual SPIONs can now be distinguished from within small aggregates. An increase in magnetic resolution allows for this technique to localize and characterize nanoscale magnetic domains with a higher degree of accuracy. It is unclear as to exactly why this occurred. It could simply be caused by variation between MFM probes and the non-homogeneous magnetic fields they produce as discussed in section 4.2. Although, the fact that this level of magnetic detail was never observed until this method was used suggests that the source of this is due to the 3-MPTS method used. Due to the fact that the mica substrates are coated with gold, it is possible that the weak diamagnetic property possessed by the gold, is somehow influencing the MFM probe to produce this high magnetic resolution.

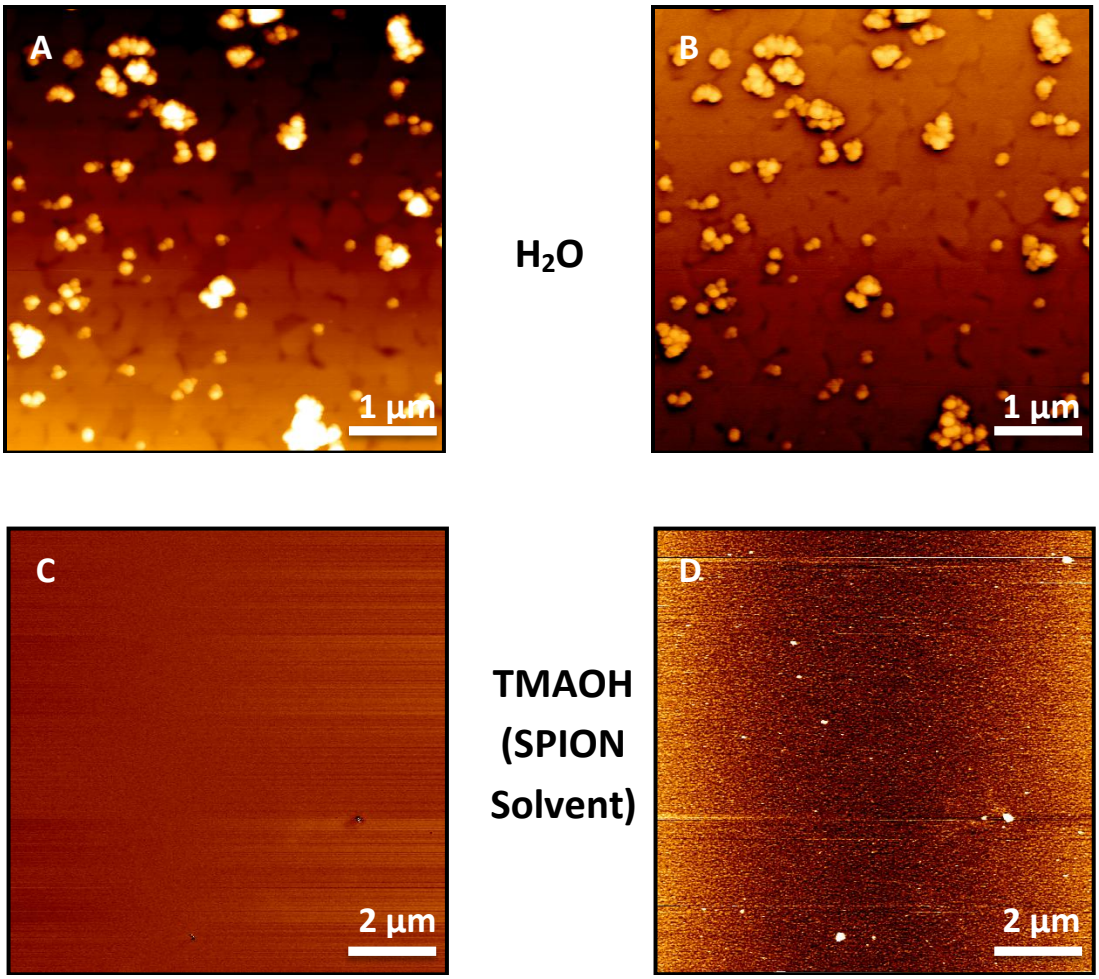

Figure 4.6. Comparison of SPIONs in water or TMAOH solvent on gold coated 3-MPTS functionalized mica. AFM topography images for SPIONs in both solvents, water (A) and TMAOH (C). MFM images for SPIONs in both solvents, water (B) and TMAOH (D). Images were taken using a magnetic AFM probe in the presence of an externally applied perpendicular magnetic field in ambient conditions. Scale bars are shown in the bottom right of each panel. Successful SPION deposition was only observed for the SPIONs in water.

With respect to the goal of this 3-MPTS method, the SPIONs in figure 4.6 were observed even after the substrates were kept in aqueous solution for an hour followed by thorough rinsing. This demonstrates the formation of the covalent bond between the SiO_2 coated SPIONs and the 3-MPTS and its ability to secure these SPIONs to a gold substrate in the presence of liquid. From figure 4.6, it can be seen that successful SPION deposition only occurred for SPIONs in a water

solvent. TMAOH has been shown to be a strong etchant of SiO_2 (~ 1nm/min), which forms the coating around the SPIONs (Laurent *et al.*, 2007). Since this etching process would have been occurring for the SPIONs in TMAOH, these particles were effectively uncoated bare SPIONs. As seen in figure 2.1, this deposition process involving 3-MPTS is dependent upon the silanol functional groups present on the SiO_2 coating of the SPIONs. Thus, with the SiO_2 coating absent, deposition via 3-MPTS will not occur.

5.0 Conclusions and Future Studies

Despite great progress and a rapidly advancing field of research there have always been problems associated with magnetic nanoparticles and their applications; overcoming immunological reactions, avoiding toxic responses to intravenously injected particles, proper clearance of particles, and the debate over whether or not to sacrifice more efficient uptake at the cost of negative side effects have been prominent issues within the field. Proper and relevant *in vitro* and ultimately *in vivo* characterization of the magnetic properties of these nanoparticles can now be added to this list.

From this thesis presented, it is evident that the advantage of MFM is its ability to spatially localize and characterize nanoscale magnetic structures with relatively limited sample preparation and without the use of labels or tags. This technique would be most effectively utilized detecting and localizing naturally occurring ferromagnetic or superparamagnetic nanoparticles in physiological systems. There are ultra-small superparamagnetic nanoparticles that naturally occur in biological systems, but there have only been a handful of studies that have reported on the possible use of MFM to detect these particles. These studies include the detection of iron compounds associated with neurological disorders (Dobson, 2001), magnetic domains in magnetotactic bacteria (Diebel *et al.*, 2000) and iron deposits in livers with Hepatitis B (Martinelli *et al.*, 2004). Proper detection and characterization of these naturally occurring nanoparticles would be met with several difficulties. Nanoparticles could be embedded, at different depths, in various biological matrices and would require detection in a fluid environment. Moreover, there are even fewer studies that report on detecting magnetic nanoparticles, specifically SPIONs, *in vitro* (Rasa *et al.*, 2002) at ambient conditions (Zhang *et al.*, 2009; Schreiber *et al.*, 2008).

Overall and in an effort to satisfy these needs, we present for the first time the use of MFM in a liquid environment on the nanoscale to detect individual SPION clusters that have been covered with hydrophobic polymers establishing the applicability of MFM as a potential technique to detect SPIONs in physiologically relevant conditions. To mimic physiological conditions, SPIONs were covered with hydrophobic polymers and imaged using MFM at various scan heights that could be encountered for intra-cellular MFM. MFM analysis of the same polymer covered SPIONs was also performed in liquid (water) to demonstrate the potential for MFM in a fluid environment that would be encountered in a biological system. The potential use of 3-MPTS to fix SiO_2 SPIONs onto gold substrates for MFM imaging in liquid was demonstrated. Individual bare and SiO_2 coated SPIONs were also compared to investigate the effect of a silica coating on the magnetic properties of SPIONs. But, in order to properly investigate the scope for MFM in detecting magnetic nanoparticles in biological systems, further study is still needed. Yet, the localization of SPIONs using MFM still offers great potential for biological applications. We hope by showing that SPIONs can be imaged with MFM in liquid when covered with hydrophobic polymers, that a more accurate and detailed understanding of the characteristics of SPIONs and magnetic nanoparticles in physiological conditions can be gained. This will allow us to understand the feasibility of detecting magnetic nanoparticles within cell membranes without any labeling or modifications and evaluate MFM as a potential magnetic analogue for fluorescence microscopy. These results could potentially lead to cell studies and encourage the development of MFM for further application in biology.

References

Albrecht, M., Janke, V., Sievers, S., Siegner, U., Schuler, D. & Heyen, U. (2005). Scanning force microscopy study of biogenic nanoparticles for medical applications. *Journal of Magnetism and Magnetic Materials, 290*, 269–271.

Alcala, M.D. & Real, C. (2006). Synthesis based on the wet impregnation method and characterization of iron and iron oxide-silica nanocomposites. *Solid State Ionics, 177*(9), 955–960.

Belliard, L. (1997). Investigation of the domain contrast in magnetic force microscopy. *Journal of Applied Physics, 81*, 3849-3851.

Bergey, E.J., Levy, L., Wang, X.P., Krebs, L.J., Lal, M., Kim, K.S., Pakatchi, S., Liebow, C. & Prasad, P.N. (2002). DC magnetic field induced magnetocytolysis of cancer cells targeted by LH-RH magnetic nanoparticles in vitro. *Biomededical Microdevices, 4*(4),293–299.

Bertorelle, F., Wilhelm, C., Roger, J., Gazeau, F., Menager, C. & Cabuil V. (2006). Fluorescence-modified superparamagnetic nanoparticles: Intracellular uptake and use in cellular imaging. *Langmuir, 22*, 5385–5391.

Choi, K.H., Lee, S.H., Kim, Y.R. Magnetic behavior of Fe3O4 nanostructure fabricated by template method. *Journal of Magnetism and Magnetic Materials, 310*(2), e861-e863.

DiCarlo, A., Scheinfein, M.R. & Chamberlin, R.V. (1992). Magnetic force microscopy utilizing an ultrasensitive vertical cantilever geometry. *Applied Physics Letters*, 61(19), 2108–2110.

Diebel, C.E., Proksch, R., Green, C.R., Neilson, P.& Walker, M.M. (2000). Magnetite defines a vertebrate magnetoreceptor. *Nature, 406*, 299–302.

Dobson, J. (2001). Nanoscale biogenic iron oxides and neurodegenerative disease. *FEBS Letters, 496*(1), 1–5.

Euliss, L.E., Grancharov, S.G., O'Brien, S., Deming, T.J., Stucky, G.D., Murray, C.B. & Held, G.A. (2003). Cooperative assembly of magnetic nanoparticles and block copolypeptides in aqueous media. *Nano Letters, 3*(11), 1489–1493.

Gong, J. & Wei, D. (2007). Comparison of micromagnetic and point probe model in magnetic force microscope simulation. *IEEE Transactions on Magnetism, 43*(10) 3821–3825.

Gupta, A.K. & Wells, S. (2004) Surface-modified superparamagnetic nanoparticles for drug delivery: Preparation, characterization, and cytotoxicity studies. *IEEE Transactions on Nanobioscience, 3*(1) 66–73.

Hartmann, U. (1999). Magnetic force microscopy, *Annual Review of Materials Science, 29*, 53-87.

Kar, M., Vijayakumar, PS., Prasad, BLV., Gupta, SS. (2010). Synthesis and Characterization of Poly-L-lysine-Grafted Silica Nanoparticles Synthesized via NCA Polymerization and Click Chemistry. *Langmuir*, **26** (8) 5772–5781.

Khollam, Y.B., Dhage, S.R., Potdar, H.S., Deshpande, S.B., Bakare, P.P., Kulkarni, S.D. & Date, S.K. (2002). Microwave hydrothermal preparation of submicron-sized spherical magnetite (Fe3O4) powders. *Materials Letters, 56* (4), 571–577.

Laurent, S., Forge, D., Port, M., Roch, A., Robic, C., Vander Elst, L., Muller, RN. (2007). Magnetic Iron Oxide Nanoparticles: Synthesis, Stabilization, Vectorization, Physicochemical Characterizations, and Biological Applications. *Chemical Reviews, 108(6),* 2064–2110.

Liu, X.Q., Xing, J., Guan, Y., Shan, G. & Liu, H.Z. (2004). Synthesis of amino-silane modified superparamagnetic silica supports and their use for protein immobilization. *Colloids and Surfaces A: Physicochemical Engineering Aspects, 238*, 127–131.

Ma, D., Guan, J., Normandin, F. (2006). Multifunctional nano-architecture for biomedical applications. *Chemistry of Materials, 18*(7), 1920–1927.

Mahmoudi, M., Sant, S., Wang, B., Laurent, S. & Sen, T. (2011). Superparamagnetic iron oxide nanoparticles (SPIONs) : Development, surface modification and applications in chemotherapy. *Advanced Drug Delivery Reviews, 63*, 24-46.

Martin, Y., Rugar, D. & Wickramasinghe, H.K. (1988). High-resolution magnetic imaging of domains in TbFe by force microscopy. *Applied Physics Letters, 52*(3):244–246.

Martin, Y. & Wickramasinghe, H.K. (1987). Magnetic imaging by force microscopy with 1000-Å resolution. *Applied Physics Letters, 50*(20),1455–1457.

Martinelli, A.L., Filho, A.B., Franco, R.F., Tavella, M.H., Ramalho, L.N., Zucoloto, S., Rodrigues, S.S.& Zago, M.A. (2004). Liver iron deposits in hepatitis B patients: Association with severity of liver disease but not with hemochromatosis gene mutations. *Journal of Gastroenterology and Hepatology, 19*(9), 1036–1041.

Miltenyi, S., Muller, W., Weichel, W. & Radbruch, A. (1990). High gradient magnetic cell separation with MACS. *Cytometry, 11*(2), 231–238.

Mironov, V. L., Nikitushkin, D.S., Bins, C., Shubin, A.B. & Zhdan, P.A. (2007). Magnetic force microscope contrast simulation for low-coercive ferromagnetic and superparamagnetic nanoparticles in an external magnetic field, *IEEE Transactions on Magnetics, 43*, 3961-3963.

Nave, R. (2009). Variations in hysteresis in magnetic materials. *Hyperphysics.* <http://hyperphysics.phy-astr.gsu.edu/hbase/solids/hyst.html>

Neves, CS., Quaresma, P., Baptista, PV., Carvalho, PA., Pedro, AJ., Pereira, E., Eaton, P. (2010). New insights into the use of magnetic force microscopy to discriminate between magnetic and nonmagnetic nanoparticles. *Nanotechnology, 21(30)*, 305706.

Pacifico, J., van Leeuwen, YM., Spuch Calvar, M., Sanchez Iglesias, A., Rodriguez Lorenzo, L., Perez Juste, J., Pastoriza Santos, I., Liz Marzan, LM. (2009). Field gradient imaging of nanoparticle systems: analysis of geometry and surface coating effects. *Nanotechnology, 20(9)*, 095708.

Park, J.W., Yoo, I.S., Chang, W.S., Lee, E.C., Ju, H., Chung, B.H. & Kim, B.S. (2008). Magnetic moment measurement of magnetic nanoparticles using atomic force microscopy. *Measurement Science and Technology*, *19*(1), 017005.

Pedreschi, F., Sturm, J.M., O'Mahony, J.D. & Flipse, C.F.J. (2003). Magnetic force microscopy and simulations of colloidal iron nanoparticles. *Journal of Applied Physics*, *94*(5), 3446–3450.

Proksch, R.B., Schaffer, T.E., Moskowitz, B.M., Dahlberg, E.D., Bazylinski, D.A. & Frankel, R.B. (1995). Magnetic force microscopy of the submicron magnetic assembly in a magnetotactic bacterium. *Applied Physics Letters*, *66*(19), 2582–2584.

Puntes, V.F., Gorostiza, P., Aruguete, D.M., Bastus, N.G., Alivisatos, A.P. (2004). Collective behaviour in two-dimensional cobalt nanoparticle assemblies observed by magnetic force microscopy. Nature Materials, 3, 263–268.

Qian, C.X., Tong, H.C., Liu, F.H., Shi, X., Dey, S., Proksch, R.B., Nielson, P. & Hachfeld, E. (1999). Characterization of high density spin valve recording heads by novel magnetic force microscope. *IEEE Transactions on Magnetics*, *35*(5), 2625–2627.

Ramlan, D.G., May, S.J., Zheng, J. G., Allen, J. E., Wessels, B.W. & Lauhon, L.J. (2006). Ferromagnetic self-assembled quantum dots on semiconductor nanowires. *Nano Letters*, *6*(1), 50–54.

Rasa, M., Kuipers, B.W.M. & Philipse A.P. (2002). Atomic force microscopy and magnetic force microscopy study of model colloids. *Journal of Colloid and Interface Science, 250*(2), 303–315.

Roiter, Y., Ornatska, M., Rammohan, AR., Balakrishnan, J., Heine, DR., Minko, Sergiy. (2009). Interaction of Lipid Membrane with Nanostructured Surfaces. Langmuir 2009, 25(11), 6287–6299

Saboktakin, M.R., Maharramov, A. & Ramazanov. M.A. (2009). Synthesis and characterization of superparamagnetic nanoparticles coated with carboxymethyl starch (CMS) for magnetic resonance imaging technique. *Carbohydrate Polymers, 78*(2), 292–295.

Schaffer, T.E., Radmacher, M. & Proksch, R. (2003). Magnetic force gradient mapping. *Journal of Applied Physics, 94*, 6525-6532.

Schwarz, A. & Wiesendanger, R. (2008). Magnetic sensitive force microscopy. *Nano Today, 3*, 28-39.

Sen, T., Magdassi, S., Nizri, G. & Bruce, I.J. (2006). Dispersion of magnetic nanoparticles in suspension. *Micro & Nano Letters,1*(1), 39–42.

Sievers, S., Albrecht, M., Siegner, U., Herweg, C. & Freyhardt, H.C. (2005). Self-ordered growth and magnetic force microscopy study of iron nanoparticles. *Journal of Applied Physics, 97*(10), 10J308–10J308-3.

Sugimoto, T. ed. (2000). Fine particles: Synthesis, characterisation and mechanism of growth. *Volume 92 of Surfactant Science Series*. Marcel Dekker, New York, New York.

Sun, S.H. & Zeng, H. (2002). Size-controlled synthesis of magnetite nanoparticies. *Journal of the American Chemical Society, 124*(28) ,8204–8205.

Sahoo, Y., Pizem, H., Fried, T., Golodnitsky, D., Burstein, L., Sukenik,C.N., Markovic, G. (2001). Alkyl phosphonate/phosphate coating on magnetite nanoparticles: A comparison with fatty acids. *Langmuir, 17*(25), 7907–7911.

Takamura, Y., Chopdekar, R.V., Scholl, A., Doran, A., Liddle, J. A., Harteneck, B. & Suzuki, Y. (2006). Tuning magnetic domain structure in nanoscale La0.7Sr0.3MnO3 Islands. *Nano Letters, 6*(6), 1287–1291.

Yacoot, A. & Koenders, L. (2008). Aspects of scanning force microscope probes and their effects on dimensional measurement. *Journal of Physics D: Applied Physics, 41*, 103001.

Zhao, X. & Harris, J.M. (1998). Novel degradable poly(ethylene glycol) hydrogels for controlled release of protein. *Journal of Pharmaceutical Sciences, 87*(11), 1450–1458.

Zhu, X.B., Grutter, P., Metlushko, V., Hao, Y., Castano, F.J., Ross, C.A., Ilic, B. Smith, H.I. (2003). Construction of hysteresis loops of single domain elements and coupled permalloy ring arrays by magnetic force microscopy. *Journal of Applied Physics, 93*(10), 8540–8542.